

Tradeoffs of Diagonal Fisher Information Matrix Estimators

Alexander Soen 

The Australian National University
RIKEN AIP
alexander.soen@anu.edu.au

Ke Sun 

CSIRO's Data61
The Australian National University
sunk@ieee.org

Abstract

The Fisher information matrix characterizes the local geometry in the parameter space of neural networks. It elucidates insightful theories and useful tools to understand and optimize neural networks. Given its high computational cost, practitioners often use random estimators and evaluate only the diagonal entries. We examine two such estimators, whose accuracy and sample complexity depend on their associated variances. We derive bounds of the variances and instantiate them in regression and classification networks. We navigate trade-offs of both estimators based on analytical and numerical studies. We find that the variance quantities depend on the non-linearity w.r.t. different parameter groups and should not be neglected when estimating the Fisher information.

1 Settings

In the parameter space of neural networks (NNs), i.e. the *neuromanifold* (Amari, 2016), the network weights and biases play the role of a coordinate system and the local metric tensor can be described by the Fisher Information Matrix (FIM). As a result, empirical estimation of the FIM helps reveal the geometry of the loss landscape during parameter learning and the intrinsic structure of the neuromanifold. Utilizing these insights has led to efficient optimization algorithms, e.g., the natural gradient (Amari, 2016) and Adam (Kingma & Ba, 2015).

A NN with inputs \mathbf{x} and stochastic outputs \mathbf{y} can be specified by the conditional probability distribution $p(\mathbf{y} | \mathbf{x}; \boldsymbol{\theta})$, where $\boldsymbol{\theta}$ is the NN weights and biases. This paper considers the general parametric form

$$p(\mathbf{y} | \mathbf{x}; \boldsymbol{\theta}) = \pi(\mathbf{y}) \cdot \exp(\mathbf{t}^\top(\mathbf{y})\mathbf{h}_\boldsymbol{\theta}(\mathbf{x}) - F(\mathbf{h}_\boldsymbol{\theta}(\mathbf{x}))), \quad (1)$$

where $\mathbf{h}_\boldsymbol{\theta} : \mathbb{R}^I \rightarrow \mathbb{R}^T$ maps I -dimensional inputs \mathbf{x} to T -dimensional exponential family parameters, $\mathbf{t}(\mathbf{y})$ is a vector of sufficient statistics, $\pi(\mathbf{y})$ is a base measure, and $F(\cdot)$ is the log-partition function (normalizing the exponential). For example, if \mathbf{y} denotes class labels and $\mathbf{t}(\mathbf{y})$ maps to its corresponding one-hot vectors, then Eq. (1) is associated with a multi-class classification network.

By assuming that the marginal data distribution $q(\mathbf{x})$ is parameter-free, we get parametric models $p(\mathbf{x}, \mathbf{y}; \boldsymbol{\theta}) = q(\mathbf{x})p(\mathbf{y} | \mathbf{x}; \boldsymbol{\theta})$ of the joint distribution. By definition, the (joint) FIM has the form $\mathcal{I}(\boldsymbol{\theta}) := \mathbb{E}_{q(\mathbf{x})} [\mathcal{I}(\boldsymbol{\theta} | \mathbf{x})]$, where

$$\mathcal{I}(\boldsymbol{\theta} | \mathbf{x}) := \mathbb{E}_{p(\mathbf{y} | \mathbf{x}; \boldsymbol{\theta})} \left[\frac{\partial \log p(\mathbf{y} | \mathbf{x}; \boldsymbol{\theta})}{\partial \boldsymbol{\theta}} \frac{\partial \log p(\mathbf{y} | \mathbf{x}; \boldsymbol{\theta})}{\partial \boldsymbol{\theta}^\top} \right] \stackrel{(*)}{=} \mathbb{E}_{p(\mathbf{y} | \mathbf{x}; \boldsymbol{\theta})} \left[\frac{\partial^2 \log p(\mathbf{y} | \mathbf{x}; \boldsymbol{\theta})}{\partial \boldsymbol{\theta} \partial \boldsymbol{\theta}^\top} \right] \quad (2)$$

is the ‘conditional FIM’ and \mathbb{E} denotes the expectation. The second equality (*) holds if the activation functions are in $C^2(\mathbb{R})$ (i.e., $\mathbf{h}_\boldsymbol{\theta}$ is a sufficiently smooth NN). $\mathcal{I}(\boldsymbol{\theta} | \mathbf{x})$ does *not* have this equivalent

expression (*) for NNs with ReLU activation functions (Soen & Sun, 2021). Both $\mathcal{I}(\boldsymbol{\theta})$ and $\mathcal{I}(\boldsymbol{\theta} | \boldsymbol{x})$ give a $\dim(\boldsymbol{\theta}) \times \dim(\boldsymbol{\theta})$ positive semi-definite (PSD) matrix. The distinction in notation is for emphasizing that the joint FIM (depending only on $\boldsymbol{\theta}$) is simply the average over individual conditional FIMs (depending on both $\boldsymbol{\theta}$ and \boldsymbol{x}).

In practice, the FIM is typically computationally expensive and needs to be estimated. Given $q(\boldsymbol{x})$ and a NN with weights and bias $\boldsymbol{\theta}$ parameterizing $p(\boldsymbol{y} | \boldsymbol{x}; \boldsymbol{\theta})$, as per Eq. (1), we consider two commonly used estimators of the FIM (Guo & Spall, 2019; Soen & Sun, 2021) given by

$$\hat{\mathcal{I}}_1(\boldsymbol{\theta}) := \frac{1}{N} \sum_{k=1}^N \left[\frac{\partial \log p(\boldsymbol{y}_k | \boldsymbol{x}_k)}{\partial \boldsymbol{\theta}} \frac{\partial \log p(\boldsymbol{y}_k | \boldsymbol{x}_k)}{\partial \boldsymbol{\theta}^\top} \right], \quad (3)$$

$$\hat{\mathcal{I}}_2(\boldsymbol{\theta}) := \frac{1}{N} \sum_{k=1}^N \left[-\frac{\partial^2 \log p(\boldsymbol{y}_k | \boldsymbol{x}_k)}{\partial \boldsymbol{\theta} \partial \boldsymbol{\theta}^\top} \right], \quad (4)$$

where we shorthand $p(\boldsymbol{y}_k | \boldsymbol{x}_k) := p(\boldsymbol{y}_k | \boldsymbol{x}_k; \boldsymbol{\theta})$ and $(\boldsymbol{x}_1, \boldsymbol{y}_1), \dots, (\boldsymbol{x}_N, \boldsymbol{y}_N)$ are i.i.d. sampled from $p(\boldsymbol{x}, \boldsymbol{y}; \boldsymbol{\theta})$. A conditional variant of the above estimators, denoted as $\hat{\mathcal{I}}_1(\boldsymbol{\theta} | \boldsymbol{x})$ and $\hat{\mathcal{I}}_2(\boldsymbol{\theta} | \boldsymbol{x})$, can be defined by fixing $\boldsymbol{x} = \boldsymbol{x}_1 = \dots = \boldsymbol{x}_N$ and sampling $\boldsymbol{y}_1, \dots, \boldsymbol{y}_N$ from $p(\boldsymbol{y} | \boldsymbol{x}; \boldsymbol{\theta})$ in Eqs. (3) and (4) — details omitted for brevity.

Both estimators are random matrices with the same shape as $\mathcal{I}(\boldsymbol{\theta})$. By Eq. (2), their means are exactly the FIM and thus they are *unbiased*¹. For the setting presented in Eq. (1), the variances of the estimators Eqs. (3) and (4) can be in closed form and upper-bounded (Soen & Sun, 2021). This provides an important tool in characterizing the accuracy of the estimators to gain insights on where/when different estimators of the FIM should be used. Despite this, neither the variance nor the bounds can be computed efficiently in practice due to the huge dimensionality of $\boldsymbol{\theta}$ in deep NNs.

This work focuses on estimating the *diagonal entries* of the FIM and their associated variance. Our main results — including the estimators of the FIM, their variances, and the bounds of the variances — can be computed efficiently through automatic differentiation and are therefore useful in practice. Our analytical results reveal how the moments of the output exponential family and how the gradients of the neural network in Eq. (1) affects the estimation of the FIM. We discover a general decomposition of the variance of the FIM corresponding respectively to the sampling of \boldsymbol{x} and \boldsymbol{y} . We further give an estimation formula that can trade-off between the bias and variance in estimating the FIM and discuss its meaning in deep learning.

2 Related Work

Prior efforts aim to analyze the structure of the FIM of neural networks with randomized weights (Amari et al., 2019). This body of work hinges on utilizing tools from random matrix theory and spectral analysis, characterizing the behavior and statistics of the FIM (Pennington & Worah, 2018). One insight is that randomly weighted neural networks have FIMs with a majority of eigenvalues close to zero; with the other eigenvalues taking large values (Karakida et al., 2019; 2021). In our work, the randomness stems from sampling from data distributions $p(\boldsymbol{y} | \boldsymbol{x}_k)$. Despite this difference, we note that our settings intersect at one point of the learning process of a neural network: the initial training iterations. Indeed, the random matrices examined in these works provide insights about the initialization of neural networks (Karakida et al., 2019). Issues for utilizing the empirical FIM to approximate the FIM have been highlighted (Pascanu & Bengio, 2014; Martens, 2020). For example, estimators of the FIM do not in general capture any second-order information about the log-likelihood (Kunstner et al., 2020).

¹Only true for $\hat{\mathcal{I}}_2(\boldsymbol{\theta})$ if activation functions are in $C^2(\mathbb{R})$.

Various structural FIM approximations have been considered to examine trade-offs between second-order information and computation (Karakida & Osawa, 2020). One can consider the *unit-wise* FIM (Ollivier, 2015; Le Roux et al., 2007; Sun & Nielsen, 2017; Amari et al., 2019), where a block-diagonal approximation of the FIM is taken to capture curvature information of intra-neuron parameter groups. Alternatively, one can study the block-diagonal *layer-wise* FIM which considers the parameter interaction within each layer (Kurita, 1994; Martens et al., 2010; Pascanu & Bengio, 2014; Martens & Grosse, 2015; Heskes, 2000; Ren & Goldfarb, 2021). Structurally, the diagonal FIM is a subset of the unit-wise FIM, which in turn is a subset of the layer-wise FIM. In the literature, a class of FIM estimators denoted as the quasi-diagonal FIM actually approximates the unit-wise FIM (Ollivier, 2015; Amari et al., 2019). Alternative to the FIM is the Generalized Gauss-Newton (GGN) matrix — a Hessian approximator — which was originally motivated through the squared loss for non-linear models (Martens, 2020). The GGN is shown to be equivalent to the FIM when a loss function is taken to be the empirical expectation of the negative log-likelihood of Eq. (1) (Heskes, 2000; Pascanu & Bengio, 2014; Martens, 2020).

The FIM estimators for NNs follow the same principle as Monte Carlo (MC) information geometry (Nielsen & Hadjeres, 2019) where information geometric quantities are approximated via MC estimation.

3 Variance of Diagonal FIM Estimators

In our notations, all vectors such as \mathbf{x} , \mathbf{y} , and $\boldsymbol{\theta}$ are column vectors. We use k to index random samples \mathbf{x} and \mathbf{y} and use i and j to index the neural network weights and biases $\boldsymbol{\theta}$. We shorthand $\mathbf{h} := \mathbf{h}_\theta$, $p(\mathbf{y} | \mathbf{x}) := p(\mathbf{y} | \mathbf{x}; \boldsymbol{\theta})$, and $p(\mathbf{y}, \mathbf{x}) := p(\mathbf{y}, \mathbf{x}; \boldsymbol{\theta})$ whenever the parameters $\boldsymbol{\theta}$ is clear from context. To be consistent, we use ‘ $| \mathbf{x}$ conditioning’ to distinguish between jointly calculated values versus conditioned values with fixed \mathbf{x} . By default, the derivatives are w.r.t. $\boldsymbol{\theta}$. For example, $\partial_i \mathbf{h} := \partial \mathbf{h} / \partial \theta_i$ and $\partial_i^2 \mathbf{h} := \partial^2 \mathbf{h} / \partial \theta_i^2$. We adopt Einstein notation to express tensor summations, so that an index appearing as both a subscript and a superscript in the same term indicates a summation. For example, $x^a y_a$ denotes $\sum_a x^a y_a$. Whenever convenient, we use a mix of standard Σ -sum and Einstein notation.

Based on the parametric form of the model in Eq. (1), the diagonal entries of the FIM estimators in Eqs. (3) and (4) can be written as follows²:

$$\hat{\mathcal{I}}_1(\theta_i) = \frac{1}{N} \sum_{k=1}^N \left(\frac{\partial F(\mathbf{h}(\mathbf{x}_k))}{\partial \theta_i} - \frac{\partial \mathbf{h}^a(\mathbf{x}_k)}{\partial \theta_i} \cdot \mathbf{t}_a(\mathbf{y}_k) \right)^2, \quad (5)$$

$$\hat{\mathcal{I}}_2(\theta_i) = \frac{1}{N} \sum_{k=1}^N \left(\frac{\partial^2 F(\mathbf{h}(\mathbf{x}_k))}{\partial^2 \theta_i} - \frac{\partial^2 \mathbf{h}^a(\mathbf{x}_k)}{\partial^2 \theta_i} \cdot \mathbf{t}_a(\mathbf{y}_k) \right). \quad (6)$$

Clearly $\hat{\mathcal{I}}_1(\theta_i) \geq 0$, while there is no such guarantee for $\hat{\mathcal{I}}_2(\theta_i)$ which can be negative.

Our results will be expressed in terms of the (central) moments of $\mathbf{t}(\mathbf{y})$:

$$\boldsymbol{\eta}_a(\mathbf{x}) := \mathbb{E}_{p(\mathbf{y} | \mathbf{x})} [\mathbf{t}_a(\mathbf{y})], \quad (7)$$

$$\mathcal{I}(\mathbf{h} | \mathbf{x}) := \mathbb{E}_{p(\mathbf{y} | \mathbf{x})} [(\mathbf{t}(\mathbf{y}) - \boldsymbol{\eta}(\mathbf{x}))(\mathbf{t}(\mathbf{y}) - \boldsymbol{\eta}(\mathbf{x}))^\top], \quad (8)$$

$$\mathcal{K}^p(\mathbf{t} | \mathbf{x}) := \mathbb{E}_{p(\mathbf{y} | \mathbf{x})} [(\mathbf{t}(\mathbf{y}) - \boldsymbol{\eta}(\mathbf{x})) \otimes (\mathbf{t}(\mathbf{y}) - \boldsymbol{\eta}(\mathbf{x})) \otimes (\mathbf{t}(\mathbf{y}) - \boldsymbol{\eta}(\mathbf{x})) \otimes (\mathbf{t}(\mathbf{y}) - \boldsymbol{\eta}(\mathbf{x}))], \quad (9)$$

where “ \otimes ” denotes the tensor product. We denote the covariance of \mathbf{t} w.r.t. to $p(\mathbf{y} | \mathbf{x})$ as $\text{Cov}^p(\mathbf{t} | \mathbf{x})$ — noting that Eq. (8) is simply $\mathcal{I}(\mathbf{h} | \mathbf{x}) = \text{Cov}^p(\mathbf{t} | \mathbf{x})$. The 4D tensor $\mathcal{K}^p(\mathbf{t} | \mathbf{x})$ denotes the 4th central

²Derivations of our formal results are provided in the appendix.

moment of $\mathbf{t}(\mathbf{y})$ w.r.t. $p(\mathbf{y} | \mathbf{x})$. These (central) moments correspond to the cummulants of $\mathbf{t}(\mathbf{y})$, *i.e.* the derivatives of F w.r.t. the natural parameters $\mathbf{h}(\mathbf{x})$ of the exponential family. Therefore, the derivatives of F in Eqs. (5) and (6) can further be written in terms of $\boldsymbol{\eta}(\mathbf{x})$ and $\mathcal{I}(\mathbf{h} | \mathbf{x})$ following the chain rule.

In practice, both estimators can be computed via automatic differentiation (Paszke et al., 2019; Dangel et al., 2019). In terms of complexity, by restricting our estimates of the FIM to just its diagonal elements, we only need to calculate $\mathcal{O}(\dim(\boldsymbol{\theta}))$ elements (originally $\mathcal{O}(\dim(\boldsymbol{\theta}) \times \dim(\boldsymbol{\theta}))$ for the full FIM). Although the log-partition function for general exponential family distributions can be complicated, for the ones used in neural networks (determined by the loss functions used in optimization) (Soen & Sun, 2021) the log-partition function F can be in closed-form; and thus the cummulants in Eqs. (7) and (8) can be calculated efficiently.

Indeed, the primary cost of the estimators comes from evaluating the gradient information of the neural network, given by $\partial \mathbf{h}(\mathbf{x}) / \partial \theta_i$ and $\partial^2 \mathbf{h}(\mathbf{x}) / \partial^2 \theta_i$. The former can be calculated easily. The latter is costly even when restricted to the diagonal elements of the FIM. With the Hessian’s quadratic complexity, in practice approximations are used to reduce the computational overhead (Becker et al., 1988; Yao et al., 2020; 2021; Elsayed & Mahmood, 2022). In this case, additional error and (potentially) variance may be introduced as a result of the Hessian approximation. It should however be noted that if we only wish to calculate the diagonal entries of the FIM for layers close the output, the cost of computing the Hessian can still be manageable. Indeed, to calculate the Hessians required for the FIM, we require all Hessian matrices (w.r.t. layer inputs) for layers closer to the output by the chain rule. As such, part of the cost can be circumvented by only considering the outermost layers. Despite this, one will still pay a cost in memory which quadratically scales with the number of parameters for non-linear activation functions (Dangel et al., 2019).

The high cost associated with the Hessian computation does not justify that $\hat{\mathcal{I}}_1$ should always be used. Such a cost can be outweighed by the FIM estimator’s variance in particular settings (choices of loss functions) (Soen & Sun, 2021). Indeed, computation is not the only determining factor for the usefulness of the estimator. This is especially true when the FIM can be used in an offline setting — where the Hessian’s cost can be tolerated — to study the singular structure of the neuromanifold (Amari et al., 2018; Sun & Nielsen, 2019), the curvature of the loss (Efron, 2018), to quantify model sensitivity (Nickl et al., 2023), and to evaluate the quality of the local optimum (Karakida et al., 2019; 2021), *etc.*

To study the quality of $\hat{\mathcal{I}}_1(\boldsymbol{\theta})$ and $\hat{\mathcal{I}}_2(\boldsymbol{\theta})$, it is natural to examine the variance of the estimators (Soen & Sun, 2021):

$$\mathcal{V}_j(\theta_i | \mathbf{x}) := \text{Var} \left(\hat{\mathcal{I}}_j(\theta_i | \mathbf{x}) \right),$$

where $\text{Var}(\cdot)$ means the variance and $\hat{\mathcal{I}}_j(\theta_i | \mathbf{x})$ ($j \in \{1, 2\}$) is defined by Eqs. (5) and (6) with $\mathbf{x} = \mathbf{x}_1 = \dots = \mathbf{x}_N$. An estimator with a smaller variance indicates that it is more accurate and more likely to be close to the true FIM. Based on the variance, one can derive sample complexity bounds of the diagonal FIM via Chebyshev’s inequality, see for instance Soen & Sun (2021, Section 3.4).

By its definition, $\mathcal{V}_j(\theta_i | \mathbf{x})$ has a simple closed form (Soen & Sun, 2021), which is detailed in Appendix A. Given a fixed $\mathbf{x} \in \mathbb{R}^I$, both $\mathcal{V}_1(\theta_i | \mathbf{x})$ and $\mathcal{V}_2(\theta_i | \mathbf{x})$ have an order of $\mathcal{O}(1/N)$, with N denoting the number of samples of \mathbf{y}_k . They further depend on two factors: ① the derivatives of the parameter-output mapping $\boldsymbol{\theta} \rightarrow \mathbf{h}$ stored in a $T \times \dim(\boldsymbol{\theta})$ matrix, either $\partial_i \mathbf{h}^a(\mathbf{x})$ or $\partial_{ii}^2 \mathbf{h}^a(\mathbf{x})$, where the latter can be expensive to calculate; and ② the central moments of $\mathbf{t}(\mathbf{y})$, whose computation only scales with T (the number of output units) and is independent to $\dim(\boldsymbol{\theta})$.

From an information geometry (Amari, 2016) perspective, $\mathcal{I}(\boldsymbol{\theta})$, $\mathcal{V}_1(\boldsymbol{\theta})$, and $\mathcal{V}_2(\boldsymbol{\theta})$ are all pullback tensors of different orders. For example, $\mathcal{I}(\boldsymbol{\theta})$ is the pullback tensor of $\mathcal{I}(\mathbf{h})$ and the singular semi-Riemannian metric (Sun & Nielsen, 2019). They induce the geometric structures of the neuromanifold (parameterized by $\boldsymbol{\theta}$) based on the corresponding low dimensional structures of the exponential family (parameterized by \mathbf{h}).

Table 1: Exponential family statistics with eigenvalue upper bounds for central moments. For the classification case, $\sigma(\mathbf{x})$ denotes the softmax value of the logit $\mathbf{h}(\mathbf{x})$. † denotes exact eigenvalues rather than upper bounds.

Learning Setting	Exponential Family	Output \mathcal{Y}	Sufficient Statistic $\mathbf{t}(\mathbf{y})$	UB $\lambda_{\max}(\mathcal{I}(\mathbf{h} \mathbf{x}))$	UB $\tilde{\lambda}_{\max}(\mathcal{K}(\mathbf{t} \mathbf{x}))$
Regression	(Isotropic) Gaussian	\mathbb{R}^T	\mathbf{y}	1^\dagger	3^\dagger
Classification	Categorical	$[C] \subset \mathbb{R}$	$(\llbracket y = 0 \rrbracket, \dots, \llbracket y = C \rrbracket)$	$\min \left\{ \frac{\sigma_{\max}(\mathbf{x})}{1 - \ \sigma(\mathbf{x})\ _2^2} \right\}$	$2 \cdot \min \left\{ \frac{\sigma_{\max}(\mathbf{x})}{1 - \ \sigma(\mathbf{x})\ _2^2} \right\}$

4 Practical Variance Estimation

To further understand the dependencies of the derivative and central moment terms, the FIM and the variance of each estimator can be bounded to strengthen intuition. First, we present simple bounds for the FIM $\mathcal{I}(\theta_i | \mathbf{x})$ and variances of estimators $\hat{\mathcal{I}}_j(\theta_i | \mathbf{x})$.

Theorem 4.1. $\forall \mathbf{x} \in \mathbb{R}^I$,

$$\|\partial_i \mathbf{h}(\mathbf{x})\|_2^2 \cdot \lambda_{\min}(\mathcal{I}(\mathbf{h} | \mathbf{x})) \leq \mathcal{I}(\theta_i | \mathbf{x}) \leq \|\partial_i \mathbf{h}(\mathbf{x})\|_2^2 \cdot \lambda_{\max}(\mathcal{I}(\mathbf{h} | \mathbf{x})), \quad (10)$$

$$\frac{1}{N} \cdot \|\partial_i \mathbf{h}(\mathbf{x})\|_2^4 \cdot \tilde{\lambda}_{\min}(\mathcal{M}) \leq \mathcal{V}_1(\theta_i | \mathbf{x}) \leq \frac{1}{N} \cdot \|\partial_i \mathbf{h}(\mathbf{x})\|_2^4 \cdot \tilde{\lambda}_{\max}(\mathcal{M}), \quad (11)$$

$$\frac{1}{N} \cdot \|\partial_{ii}^2 \mathbf{h}(\mathbf{x})\|_2^2 \cdot \lambda_{\min}(\mathcal{I}(\mathbf{h} | \mathbf{x})) \leq \mathcal{V}_2(\theta_i | \mathbf{x}) \leq \frac{1}{N} \cdot \|\partial_{ii}^2 \mathbf{h}(\mathbf{x})\|_2^2 \cdot \lambda_{\max}(\mathcal{I}(\mathbf{h} | \mathbf{x})), \quad (12)$$

where $\mathcal{M} = \mathcal{K}^p(\mathbf{t} | \mathbf{x}) - \mathcal{I}(\mathbf{h} | \mathbf{x}) \otimes \mathcal{I}(\mathbf{h} | \mathbf{x})$; $\lambda_{\min}(\cdot) / \lambda_{\max}(\cdot)$ denotes the minimum / maximum matrix eigenvalue; and given a 4-dimensional tensor $\mathcal{T} \in \mathbb{R}^{T \times T \times T \times T}$, $\tilde{\lambda}_{\min}(\mathcal{T})$ and $\tilde{\lambda}_{\max}(\mathcal{T})$ are solutions to the following variational equations:

$$\begin{aligned} \tilde{\lambda}_{\min}(\mathcal{T}) &= \inf_{\mathbf{u}: \|\mathbf{u}\|_2=1} \mathbf{u}^a \mathbf{u}^b \mathbf{u}^c \mathbf{u}^d \mathcal{T}_{abcd}, \\ \tilde{\lambda}_{\max}(\mathcal{T}) &= \sup_{\mathbf{u}: \|\mathbf{u}\|_2=1} \mathbf{u}^a \mathbf{u}^b \mathbf{u}^c \mathbf{u}^d \mathcal{T}_{abcd}. \end{aligned} \quad (13)$$

To help ground Theorem 4.1, in Table 1, we summarize different sufficient statistics quantities for common learning settings — with further learning setting implications presented in Section 5. We further note that Eqs. (11) and (12) (and many subsequent results) can be further generalized for the variance of off-diagonal elements, see Appendix B. In this generalization, the exact form of the eigenvalue / spectral quantities change, but the dependence on the neural network weights split according the FIM coordinate, *i.e.*, in Eq. (11) $\|\partial_i \mathbf{h}(\mathbf{x})\|_2^4$ becomes $\|\partial_i \mathbf{h}(\mathbf{x})\|_2^2 \cdot \|\partial_j \mathbf{h}(\mathbf{x})\|_2^2$ and in Eq. (12) $\|\partial_{ii}^2 \mathbf{h}(\mathbf{x})\|_2^2$ becomes $\|\partial_{ij}^2 \mathbf{h}(\mathbf{x})\|_2^2$.

We stress that the values $\tilde{\lambda}_{\min}(\mathcal{T})$ and $\tilde{\lambda}_{\max}(\mathcal{T})$ in Eq. (13) correspond to tensor eigenvalues if and only if \mathcal{T} is a supersymmetric tensor (Lim, 2005) (aka totally symmetric tensor), *i.e.*, if its indices are permutation invariant. In this case, Eq. (13) is exactly the definition of the maximum and minimum Z-eigenvalues. The variational form mirrors the Courant-Fischer min-max theorem for finding the eigenvalues of symmetric matrices (Tao, 2012). In the case of Eq. (11), with $\mathcal{M} = \mathcal{K}^p(\mathbf{t} | \mathbf{x}) - \mathcal{I}(\mathbf{h} | \mathbf{x}) \otimes \mathcal{I}(\mathbf{h} | \mathbf{x})$, the tensor is not a supersymmetric tensor in general. Despite this, we note that the lower bound of Eq. (11) is non-trivial.

Nevertheless, a weaker bound as compared to Eq. (11) can be established based on the tensor Z-eigenvalue.

Corollary 4.2. $\forall \mathbf{x} \in \mathfrak{R}^I$,

$$\tilde{\lambda}_{\min}(\mathcal{K}^p(\mathbf{t} | \mathbf{x}) - \mathcal{I}(\mathbf{h} | \mathbf{x}) \otimes \mathcal{I}(\mathbf{h} | \mathbf{x})) \geq \max\left\{0, \tilde{\lambda}_{\min}(\mathcal{K}^p(\mathbf{t} | \mathbf{x})) - \lambda_{\max}^2(\mathcal{I}(\mathbf{h} | \mathbf{x}))\right\}; \quad (14)$$

$$\tilde{\lambda}_{\max}(\mathcal{K}^p(\mathbf{t} | \mathbf{x}) - \mathcal{I}(\mathbf{h} | \mathbf{x}) \otimes \mathcal{I}(\mathbf{h} | \mathbf{x})) \leq \tilde{\lambda}_{\max}(\mathcal{K}^p(\mathbf{t} | \mathbf{x})) - \lambda_{\min}^2(\mathcal{I}(\mathbf{h} | \mathbf{x})). \quad (15)$$

The tensor eigenvalue is typically expensive to calculate. However in our case, the eigenvalues $\tilde{\lambda}_{\min}(\mathcal{K}^p(\mathbf{t} | \mathbf{x}))$ and $\tilde{\lambda}_{\max}(\mathcal{K}^p(\mathbf{t} | \mathbf{x}))$ on the RHS of Eqs. (14) and (15) can be calculated via [Kolda & Mayo \(2014\)](#)'s method with $\mathcal{O}(T^4/4!)$ complexity. In this paper, we assume T is reasonably bounded and are mainly concerned with the complexity w.r.t. $\dim(\boldsymbol{\theta})$. From this perspective, all our bounds scale linearly w.r.t. $\dim(\boldsymbol{\theta})$, and thus can be computed efficiently.

When $\mathbf{t}(y) - \boldsymbol{\eta}(\mathbf{x})$ is bounded (e.g. in classification), we can upper bound $\tilde{\lambda}_{\max}(\mathcal{K}^p(\mathbf{t} | \mathbf{x}))$ with $\lambda_{\max}(\mathcal{I}(\mathbf{h} | \mathbf{x}))$, which is easier to calculate.

Proposition 4.3. Suppose $\|\mathbf{t}(y) - \boldsymbol{\eta}(\mathbf{x})\|_2^2 \leq B$. Then,

$$\tilde{\lambda}_{\max}(\mathcal{K}^p(\mathbf{t} | \mathbf{x})) \leq B \cdot \lambda_{\max}(\mathcal{I}(\mathbf{h} | \mathbf{x})) \leq B^2. \quad (16)$$

It should be noted that as long as the sufficient statistics is bounded $\|\mathbf{t}\|_2$, we have that $B = 4 \cdot \|\mathbf{t}\|_2^2 < \infty$. A similar lower bound (without bounded assumption) can be established for the minimum tensor eigenvalue $\tilde{\lambda}_{\min}(\mathcal{K}^p(\mathbf{t} | \mathbf{x})) \geq \lambda_{\min}^2(\mathcal{I}(\mathbf{h} | \mathbf{x}))$, but this ends up being trivial when applying Corollary 4.2's lower bound, Eq. (14).

One can observe a number of trade-offs by examining Theorem 4.1. An immediate observation is that the first order gradients of $\mathbf{h}(\mathbf{x})$ correspond to the robustness of \mathbf{h} to parameter misspecification (w.r.t. an input \mathbf{x}). As such, from the bounds of Eqs. (10) and (12), the scale of $\mathcal{I}(\theta_i | \mathbf{x})$ and $\mathcal{V}_2(\theta_i | \mathbf{x})$ will be large when small shifts in parameter space yield large changes in the output $\mathbf{h}(\mathbf{x})$. Another observation is how the scale of the minimum and maximum eigenvalues of $\mathcal{I}(\mathbf{h} | \mathbf{x})$ affects the scale of $\mathcal{I}(\theta_i | \mathbf{x})$ and the estimator variances. In particular, when $\lambda_{\min}(\mathcal{I}(\mathbf{h} | \mathbf{x}))$ increases, the scale of $\mathcal{V}_1(\theta_i | \mathbf{x})$ decreases but the scale of $\mathcal{I}(\theta_i | \mathbf{x})$ and $\mathcal{V}_2(\theta_i | \mathbf{x})$ increases. When $\lambda_{\max}(\mathcal{I}(\mathbf{h} | \mathbf{x}))$ decreases, then the opposite scaling occurs. With these two observations, there is a tension in how the scale of $\mathcal{I}(\theta_i | \mathbf{x})$ follows the different variances $\mathcal{V}_1(\theta_i | \mathbf{x})$ and $\mathcal{V}_2(\theta_i | \mathbf{x})$. The element-wise FIM follows $\mathcal{V}_1(\theta_i | \mathbf{x})$ in terms of the scale of neural network derivatives $\|\partial_i \mathbf{h}(\mathbf{x})\|_2$; however, the element-wise FIM follows $\mathcal{V}_2(\theta_i | \mathbf{x})$ in terms of the spectrum of sufficient statistics moment $\mathcal{I}(\mathbf{h} | \mathbf{x})$.

Remark 4.4. Typically, \mathbf{h} is the linear output units: $\mathbf{h}(\mathbf{x}) = \mathbf{W}_{-1} \mathbf{h}_{-1}(\mathbf{x})$, where \mathbf{W}_{-1} is the weights of the last layer, and $\mathbf{h}_{-1}(\mathbf{x})$ is the second last layer's output. We have $\mathcal{V}_2(\theta_i | \mathbf{x}) = 0 \leq \mathcal{V}_1(\theta_i | \mathbf{x})$ for any θ_i in \mathbf{W}_{-1} . A smaller variance $\mathcal{V}_2(\theta_i | \mathbf{x})$ is guaranteed for the last layer regardless of the choice of the exponential family in Eq. (1).

Remark 4.5. The neural network mapping w.r.t. the j 'th neuron in the second last layer is $\mathbf{h}(\mathbf{x}) = \mathbf{w}_{-1}^j \phi(\mathbf{h}_{-2}^\top(\mathbf{x}) \mathbf{w}_{-2}^j + C_{-2}) + \mathbf{c}_{-1}$, where \mathbf{w}_{-2}^j and \mathbf{w}_{-1}^j are incoming and outgoing links of the interested neuron, respectively; $\mathbf{h}_{-2}(\mathbf{x})$ is the output of the third last layer; and ϕ is the activation function. The 'constants' C_{-2} and \mathbf{c}_{-1} denote an aggregation of all terms which are independent of \mathbf{w}_{-2}^j and \mathbf{w}_{-1}^j in their respective layers. The diagonal Hessian w.r.t. \mathbf{w}_{-2}^j is $\partial^2 \mathbf{h}(\mathbf{x}) = \mathbf{w}_{-1}^j \phi''(\mathbf{h}_{-2}^\top(\mathbf{x}) \mathbf{w}_{-2}^j + C_{-2}) (\mathbf{h}_{-2}(\mathbf{x}) \circ \mathbf{h}_{-2}(\mathbf{x}))^\top$. By Theorem 4.1, $\mathcal{V}_2(\theta_i | \mathbf{x})$ can be arbitrarily small depending on $\phi''(\mathbf{h}_{-2}^\top(\mathbf{x}) \mathbf{w}_{-2}^j + C_{-2})$. For example, if $\phi(t) = 1/(1 + \exp(-t))$, then $\phi''(t) = \phi(t)(1 - \phi(t))(1 - 2\phi(t))$. In this case, for a neuron in the second last layer, a sufficient condition for $\mathcal{V}_2(\theta_i | \mathbf{x}) = 0$ (and having $\hat{\mathcal{I}}_2$ favored against $\hat{\mathcal{I}}_1$) is for the neuron's pre-activation value $\mathbf{h}_{-2}^\top(\mathbf{x}) \mathbf{w}_{-2}^j + C_{-2} = 0$. When the pre-activation value is saturated ($-\infty / \infty$), we also have that $\mathcal{V}_1(\theta_i | \mathbf{x}) = \mathcal{V}_2(\theta_i | \mathbf{x}) = 0$. Alternatively, suppose that $\phi(t) = \text{SoftPlus}(t) := \log(1 + \exp(t))$, a continuous relaxation of ReLU, then $\phi''(t) = \phi'(t)(1 - \phi'(t))$ where $\phi'(t) = 1/(1 + \exp(-t))$. As such, for a neuron in the second last layer, a sufficient condition for $\mathcal{V}_2(\theta_i | \mathbf{x}) = 0$ with $\mathcal{V}_1(\theta_i | \mathbf{x}) \neq 0$, is when $\mathbf{h}_{-2}^\top(\mathbf{x}) \mathbf{w}_{-2}^j + C_{-2} \rightarrow \infty$.

These observations can be further clarified by taking a look at these quantities over multiple parameters. So far we have only examined the variance of the FIM element-wise w.r.t. to the parameters of \mathbf{h} . To study all parameters jointly, we consider the *trace variances* of the FIM estimators: for any $j \in \{1, 2\}$, $\mathcal{V}_j(\boldsymbol{\theta} | \mathbf{x})$ denotes the trace of the covariance matrix of $\text{diag}(\hat{\mathcal{I}}_j(\boldsymbol{\theta} | \mathbf{x}))$, where $\text{diag}(\cdot)$ extracts the diagonal elements of the matrix into a column vector. In what follows, we present upper bounds of these joint quantities.

Corollary 4.6. *For any $\mathbf{x} \in \mathbb{R}^J$,*

$$\text{tr}(\mathcal{I}(\boldsymbol{\theta} | \mathbf{x})) \leq \|\partial\mathbf{h}(\mathbf{x})\|_F \cdot \min \{ \text{tr}(\mathcal{I}(\mathbf{h} | \mathbf{x})), \|\partial\mathbf{h}(\mathbf{x})\|_F \cdot \lambda_{\max}(\mathcal{I}(\mathbf{h} | \mathbf{x})) \}; \quad (17)$$

$$\mathcal{V}_1(\boldsymbol{\theta} | \mathbf{x}) \leq \frac{1}{N} \cdot \|\partial\mathbf{h}(\mathbf{x})\|_F^2 \cdot \min \left\{ \sum_{t,u=1}^T \mathcal{K}_{ttuu}^p(\mathbf{t} | \mathbf{x}) - \|\mathcal{I}(\mathbf{h} | \mathbf{x})\|_F^2, \|\partial\mathbf{h}(\mathbf{x})\|_F^2 \cdot \tilde{\lambda}_{\max}(\mathcal{M}) \right\}; \quad (18)$$

$$\mathcal{V}_2(\boldsymbol{\theta} | \mathbf{x}) \leq \frac{1}{N} \cdot \|\text{dHes}(\mathbf{h} | \mathbf{x})\|_F \cdot \min \{ \text{tr}(\mathcal{I}(\mathbf{h} | \mathbf{x})), \|\text{dHes}(\mathbf{h} | \mathbf{x})\|_F \cdot \lambda_{\max}(\mathcal{I}(\mathbf{h} | \mathbf{x})) \}, \quad (19)$$

where $\|\cdot\|_F$ denotes the Frobenius norm and $\text{dHes}(\mathbf{h} | \mathbf{x}) = (\text{diag}(\text{Hes}(\mathbf{h}_1 | \mathbf{x})), \dots, \text{diag}(\text{Hes}(\mathbf{h}_T | \mathbf{x})))$.

This upper bound comes from a combination of simply integrating the parameter-wise variances in Theorem 4.1 and incorporating an alternative trace variance bound which takes into account the full spectrum of the network derivatives and sufficient statistics quantities, full depicted in Theorem C.1. Lower bounds can also be derived in terms of singular values, we leave these to the Appendix for conciseness. We also note that the upper bound shown in Corollary 4.6 can also be improved by expressing the first term of the min function as singular value quantities.

Having the min function in Corollary 4.6 can be helpful as it shows a trade-off in two different upper bounds: the scale of the network derivatives $\partial\mathbf{h}(\mathbf{x})$ and $\partial^2\mathbf{h}(\mathbf{x})$ with the spectrum of the sufficient statistics terms. In the case of Eqs. (17) and (19), the trace of the $\mathcal{I}(\mathbf{h} | \mathbf{x})$ is exactly the sum of all eigenvalues, including $\lambda_{\max}(\mathcal{I}(\mathbf{h} | \mathbf{x}))$. This can be helpful as an alternative bound when the scale of the network derivatives are not guaranteed to be bounded by a small value. It should be noted, that by the chain rule, the scale of these network derivatives directly scale with the overall sharpness / flatness (Li et al., 2018) of the network which is associated with the derivatives of the loss function, *i.e.*, the log-likelihood of Eq. (1). For networks with large network derivative, the first term of the min is preferred to prevent quadratic scaling of $\|\partial\mathbf{h}(\mathbf{x})\|$. On the other hand, if the sharpness of the network \mathbf{h} can be controlled, *e.g.* via sharpness aware minimization (Foret et al., 2020), then the second term of the min might be preferred to avoid considering the full spectrum of $\mathcal{I}(\mathbf{h} | \mathbf{x})$ in the bound.

4.1 Joint FIM Estimators

In the above, we considered the variance of conditional FIMs, which can scale differently depending on the input \mathbf{x} . Nevertheless, the ‘joint FIM’ estimators $\hat{\mathcal{I}}_j(\theta_i)$ depend on sampling of \mathbf{x} w.r.t. the data distribution $q(\mathbf{x})$. The bounds presented in Eq. (10) can be extended to the joint FIM $\mathcal{I}(\theta_i) := \mathbb{E}_{q(\mathbf{x})} \mathcal{I}(\theta_i | \mathbf{x})$ by simply taking an expectation $\mathbb{E}_{q(\mathbf{x})}$ uniformly over the bounds. To analysis the variances of the joint FIM estimators $\mathcal{V}_j(\theta_i)$, we present the following theorem which connects the prior results established for $\mathcal{V}_j(\theta_i | \mathbf{x})$, *e.g.* Theorem 4.1, via the law of total variance.

Theorem 4.7. *For $j \in \{1, 2\}$,*

$$\mathcal{V}_j(\theta_i) = \frac{1}{N} \cdot \text{Var}(\mathcal{I}(\theta_i | \mathbf{x})) + \mathbb{E}_{q(\mathbf{x})} [\mathcal{V}_j(\theta_i | \mathbf{x})], \quad (20)$$

where $\text{Var}(\mathcal{I}(\theta_i | \mathbf{x}))$ is the variance of $\mathcal{I}(\theta_i | \mathbf{x})$ w.r.t. $q(\mathbf{x})$ and N is the number of samples of $\mathbf{y} \sim p(\mathbf{y} | \mathbf{x})$ for each \mathbf{x} .

The variance incurred when estimating the FIM has two components. The first term on the RHS of Eq. (20) characterizes the randomness of the FIM w.r.t. $q(\mathbf{x})$, or the input randomness. It vanishes when the FIM is estimated by taking the expectation w.r.t. $q(\mathbf{x})$, or the number of samples \mathbf{x}_k is large enough. The second term is caused by the sampling of \mathbf{y}_k according to $p(\mathbf{y} | \mathbf{x})$, or the output randomness, which scales with the central moments of $\mathbf{t}(\mathbf{y})$. If the network is trained so that $p(\mathbf{y} | \mathbf{x})$ tends to be deterministic, this term will disappear leaving the first term to dominate.

Eq. (20) can be further generalized using the law of total covariance to extend prior work considering conditional FIM covariances (Soen & Sun, 2021) to joint FIM covariances.

Notably, Theorem 4.7 connects the variance of assuming a fixed input \mathbf{x} with multiple samples \mathbf{y}_k with the variance of pairs of samples $(\mathbf{x}_k, \mathbf{y}_k)$. The bounds for $\mathcal{V}_j(\theta_i | \mathbf{x})$ explored in this section can thus be applied to the corresponding joint variance $\mathcal{V}_j(\theta_i)$ by using this theorem. This is straightforward and omitted.

The first variance term of Theorem 4.7 cannot be computed in practice: it relies on how the closed-form FIM varies w.r.t. the input distribution $q(\mathbf{x})$. As such, it is useful to bound the first term into computable quantities.

Lemma 4.8. $\text{Var}(\mathcal{I}(\theta_i | \mathbf{x})) \leq \mathbb{E}_{q(\mathbf{x})} [\|\partial_i \mathbf{h}(\mathbf{x})\|_2^4 \cdot \lambda_{\max}^2(\mathcal{I}(\mathbf{h} | \mathbf{x}))].$

One may notice that this upper bound is very similar to the 4th central moment term $\lambda_{\max}(\mathcal{K}^p(\mathbf{t} | \mathbf{x}))$ when considering the upper bound of estimator variance $\mathcal{V}_2(\theta_i | \mathbf{x})$ when applying Theorem 4.1 and Corollary 4.2. As such, one may wonder when $\lambda_{\max}^2(\mathcal{I}(\mathbf{h} | \mathbf{x}))$ and $\mathcal{K}_{\max}^p(\mathbf{t} | \mathbf{x})$ are equivalent. The equality $\lambda_{\max}^2(\mathcal{I}(\mathbf{h} | \mathbf{x})) = \mathcal{K}_{\max}^p(\mathbf{t} | \mathbf{x})$ holds iff $p(\mathbf{y} | \mathbf{x})$ does not depend on the outputs of $\mathbf{h}(\mathbf{x})$. Thus in our case, where a neural network parameterizes our exponential family, these eigenvalues will be distinct.

In terms of sample complexity of the joint variance, the complexity scales inversely to the joint number of samples. For instance, assuming that we take empirical expectations with N_x samples (or that $q(\mathbf{x})$ consists of the sum of Dirac delta functions) and each \mathbf{x} generates N_y samples of $\mathbf{y} \sim p(\mathbf{y} | \mathbf{x})$, using Theorem 4.7 and Lemma 4.8, then the bound sample complexity is $\mathcal{O}(1/(N_x N_y))$.

5 Case Studies

To make the implications of our theoretic results more concrete, we consider two common settings in supervised learning: regression and classification, which corresponds respectively to specifying the exponential family distribution in Eq. (1) as a multi-dimensional isotropic Gaussian distribution or a categorical distribution. We also show empirical evidence drawn from an MNIST classifier network.

5.1 Regression: Isotropic Gaussian Distribution

Consider the family of multi-dimensional isotropic Gaussian distribution. As per Eq. (1), we have $\mathbf{t}(\mathbf{y}) = \mathbf{y} \in \mathbb{R}^T$ and base measure $\pi(\mathbf{y}) \propto \exp(-\frac{1}{2}\mathbf{y}^\top \mathbf{y})$. This corresponds to the case where $\mathbf{h}(\mathbf{x})$ is trained via the squared loss. The corresponding central moments of $\mathbf{t}(\mathbf{y})$ are:

$$\begin{aligned} \mathcal{I}(\mathbf{h} | \mathbf{x}) &= \mathbf{I}; \text{ and} \\ \mathcal{K}_{abcd}^p(\mathbf{t} | \mathbf{x}) &= \mathcal{I}_{ab}(\mathbf{h} | \mathbf{x}) \cdot \mathcal{I}_{cd}(\mathbf{h} | \mathbf{x}) + \mathcal{I}_{ac}(\mathbf{h} | \mathbf{x}) \cdot \mathcal{I}_{bd}(\mathbf{h} | \mathbf{x}) + \mathcal{I}_{ad}(\mathbf{h} | \mathbf{x}) \cdot \mathcal{I}_{bc}(\mathbf{h} | \mathbf{x}). \end{aligned}$$

The derivatives of the corresponding log-partition function $F(\mathbf{h})$ yields these central moments (Soen & Sun, 2021, Lemma 5). To apply Theorem 4.1, we examine the extreme eigenvalues of $\mathcal{I}(\mathbf{h} | \mathbf{x})$ and $\mathcal{K}^p(\mathbf{t} | \mathbf{x}) - \mathcal{I}(\mathbf{h} | \mathbf{x}) \otimes \mathcal{I}(\mathbf{h} | \mathbf{x})$.

Proposition 5.1. *Suppose that the exponential family in Eq. (1) is an isotropic Gaussian distribution. Then:*

$$\begin{aligned}\lambda_{\min}(\mathcal{I}(\mathbf{h} | \mathbf{x})) &= \lambda_{\max}(\mathcal{I}(\mathbf{h} | \mathbf{x})) = 1; \\ \tilde{\lambda}_{\min}(\mathcal{K}^p(\mathbf{t} | \mathbf{x}) - \mathcal{I}(\mathbf{h} | \mathbf{x}) \otimes \mathcal{I}(\mathbf{h} | \mathbf{x})) &= 2; \\ \tilde{\lambda}_{\max}(\mathcal{K}^p(\mathbf{t} | \mathbf{x}) - \mathcal{I}(\mathbf{h} | \mathbf{x}) \otimes \mathcal{I}(\mathbf{h} | \mathbf{x})) &= 2.\end{aligned}$$

In the case of an isotropic Gaussian distribution, the eigenvalues of both sufficient statistics quantities for our bounds are equal. As such the bound for $\mathcal{I}(\theta_i | \mathbf{x})$, $\hat{\mathcal{I}}_1(\mathbf{h} | \mathbf{x})$, and $\hat{\mathcal{I}}_2(\mathbf{h} | \mathbf{x})$ in Theorem 4.1 are all equalities for standard regression.

As $\mathcal{I}(\theta_i | \mathbf{x})$ can be written exactly in terms of the gradients of \mathbf{h} , in practice one does not need to utilize a random estimator when computing the conditional FIM. Indeed, the conditional FIM simplifies to a Gauss-Newton matrix for the squared loss (Martens, 2020). When computing the FIM over a random sample \mathbf{x} , a variance still appears due to Theorem 4.7. Utilizing Lemma 4.8 and Proposition 5.1, the variance over a joint distribution is bounded by a function of the derivative $\partial_i \mathbf{h}(\mathbf{x})$ over the marginal input distributions:

$$\mathcal{V}(\theta_i) \leq \mathbb{E}_{q(\mathbf{x})} [\|\partial_i \mathbf{h}(\mathbf{x})\|_2^4] \leq \max_{\mathbf{x} \in \text{Supp}(q)} \|\partial_i \mathbf{h}(\mathbf{x})\|_2^4.$$

In other words, the overall variance to approximate the joint FIM is bounded by the gradients of the network outputs.

5.2 Classification: Categorical Distribution

For multi-class classification, we instantiate our exponential family with a categorical distribution (with unit base measure $\pi(y) = 1$). This corresponds to training a classifier network with log-loss. Let $\mathcal{Y} = [C]$ for $T = C$ classes defining the possible labels. Let $\mathbf{t}(y) = (\llbracket y = 1 \rrbracket, \llbracket y = 2 \rrbracket, \dots, \llbracket y = C \rrbracket)$, where $\llbracket r \rrbracket = 1$ when the predicate r is true and $\llbracket r \rrbracket = 0$ otherwise. Noting our results do not depend on minimal sufficiency, this $\mathbf{t}(y)$ is sufficient but *not minimal* sufficient. In this setting, the neural network outputs \mathbf{h} correspond to the logits of the label probabilities. The resulting probabilities $p(y | \mathbf{x})$ is the softmax values of \mathbf{h} denoted by $\sigma(\mathbf{x}) := \text{SoftMax}(\mathbf{h}(\mathbf{x})) \in [0, 1]^T$.

Under this setting, we have $\mathcal{I}(\mathbf{h} | \mathbf{x}) = \text{diag}(\sigma(\mathbf{x})) - \sigma(\mathbf{x})\sigma(\mathbf{x})^\top$, whose eigenvalues do not follow a convenient pattern as the number of classes C increases (Withers & Nadarajah, 2014). Likewise, the general structure of $\mathcal{K}(\mathbf{t} | \mathbf{x})$ does not provide a convenient equation for the maximum tensor eigenvalue. As such, we provide upper bounds for the maximum eigenvalues of $\mathcal{I}(\mathbf{h} | \mathbf{x})$ and $\mathcal{K}^p(\mathbf{t} | \mathbf{x}) - \mathcal{I}(\mathbf{h} | \mathbf{x}) \otimes \mathcal{I}(\mathbf{h} | \mathbf{x})$ using Corollary 4.2 and Proposition 4.3.

Theorem 5.2. *Suppose that the exponential family in Eq. (1) is a categorical distribution. With $\sigma_{\max}(\mathbf{x}) = \max_k \sigma_k(\mathbf{x})$:*

$$\begin{aligned}\lambda_{\max}(\mathcal{I}(\mathbf{h} | \mathbf{x})) &\leq m(\mathbf{x}), \\ \lambda_{\max}(\mathcal{K}^p(\mathbf{t} | \mathbf{x}) - \mathcal{I}(\mathbf{h} | \mathbf{x}) \otimes \mathcal{I}(\mathbf{h} | \mathbf{x})) &\leq 2 \cdot m(\mathbf{x}),\end{aligned}$$

where $m(\mathbf{x}) := \min(\sigma_{\max}(\mathbf{x}), 1 - \|\sigma(\mathbf{x})\|_2^2)$.

The upper bounds of Theorem 5.2 provide a tension. When the first term of $m(\mathbf{x})$ is maximized, the second is at its minimum, and vice-versa. In particular, the term that determines the upper bound depends on the uncertainty of the network's output. When the network's output is near random, *e.g.* at initialization, the first term will dominate with $\sigma_{\max}(\mathbf{x}) \approx 1/C$. However, as the network becomes more certain with its prediction, the second term will start dominating: a more deterministic output $p(y | \mathbf{x}) \rightarrow 1$ implies that $\lambda_{\max}(\mathcal{I}(\mathbf{h} | \mathbf{x})) \rightarrow 0$.

5.3 Empirical Verification: Classification

We experiment on the MNIST digit classification dataset (Deng, 2012) and a multilayer perceptron (MLP) consisting of 4 densely connected layers, sigmoid activation, and a dropout layer. The classification setting corresponds to using the categorical distribution with $C = 10$ class labels. For a random \mathbf{x} from the test set, we compute both estimators $\hat{\mathcal{I}}_1(\boldsymbol{\theta} | \mathbf{x})$ and $\hat{\mathcal{I}}_2(\boldsymbol{\theta} | \mathbf{x})$ using $N = 5,000$ samples. We record the variances of each estimator and compute their bounds based on Theorem 4.1. The Fisher information of each individual parameter and its variances are aggregated based on the arithmetic average over each of 4 parameter groups (corresponding to the 4 layers) and examined throughout 20 training epochs.

In Fig. 1, we present the variance scale of the estimators $\hat{\mathcal{I}}_1(\theta_i | \mathbf{x})$ and $\hat{\mathcal{I}}_2(\theta_i | \mathbf{x})$ in log-space; and the tightness of the bounds in Theorem 4.1 by consider the log-ratio $\log \frac{\text{UB}}{\mathcal{V}_1(\theta_i | \mathbf{x})}$, where UB is the upper bounds in Theorem 4.1. In this experiment, the UB is much tighter than the lower bound (LB), which is omitted in the figures for better clarity. More experimental results are given in Appendix E.

We varied the network architecture and the activation function. Across different settings, the proposed UB and LB are always valid. In Fig. 1, one can observe that the diagonal FIM and the associated variances have a small magnitude. For example, in the first layer, $\mathcal{V}_1(\theta_i | \mathbf{x})$ and $\mathcal{V}_2(\theta_i | \mathbf{x})$ are roughly $e^{-10} \approx 5 \times 10^{-5}$. The log-ratio $\log \frac{\text{UB}}{\mathcal{V}_1(\theta_i | \mathbf{x})} \approx 4$, meaning that UB is roughly 50 times larger than $\mathcal{V}_1(\theta_i | \mathbf{x})$. Comparatively, $\mathcal{V}_2(\theta_i | \mathbf{x})$ has a tighter UB which is 20 times larger than itself. The UB serves as a useful hint on the *order of magnitude* of the variances. In Appendix C, we present tighter bounds which are more expensive to compute.

In the first 3 layers of the MLP, $\mathcal{V}_1(\theta_i | \mathbf{x})$ presents a smaller value than $\mathcal{V}_2(\theta_i | \mathbf{x})$, meaning that $\hat{\mathcal{I}}_1$ can more accurately estimate the diagonal FIM. Interestingly, this is not true for the last layer: $\mathcal{V}_2(\theta_i | \mathbf{x})$ becomes zero while $\hat{\mathcal{I}}_1$ presents the largest variance across all parameter groups and close to the scale of the Fisher information. Due to this, one should always prefer $\hat{\mathcal{I}}_2$ over $\hat{\mathcal{I}}_1$ for the last layer. In the last two layers, $\hat{\mathcal{I}}_2$ is in simple closed form without need of automatic differentiation (see Remark 4.4).

The shape of the variance curves are sensitive to choices of the activation functions ϕ and inputs \mathbf{x} . In general, the first few epochs of the variance present more dynamics than the rest of the training process. If one uses log-sigmoid activations $\phi(t) = -\log(1 + \exp(-t))$ (which is equivalent to $\phi(t) = -\text{SoftPlus}(-t)$, as per Remark 4.4), the variances of $\hat{\mathcal{I}}_1$ and $\hat{\mathcal{I}}_2$ only appear at the randomly initialized network and quickly vanish once training starts, as shown in Appendix E. In this case, the learner more

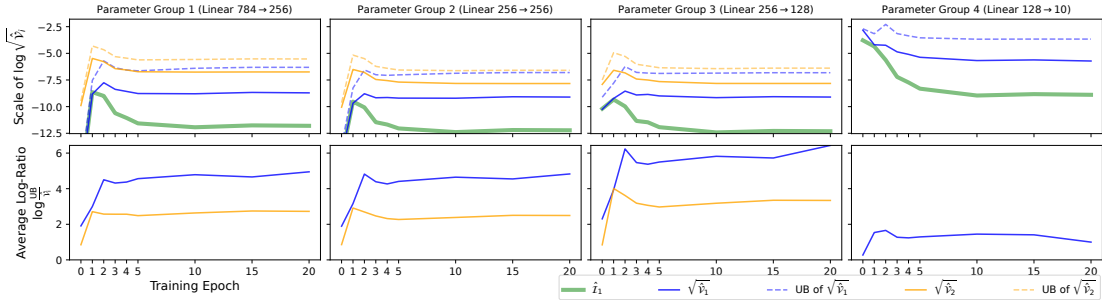


Figure 1: MNIST FIM quantities for a 4-layer MLP utilizing sigmoid activation functions. Top: The estimated Fisher information, its variances, and the bounds of the variances across 4 parameter groups and 20 training epochs. The Fisher information (the thick green line) is estimated based on $\hat{\mathcal{I}}_1$ ($\hat{\mathcal{I}}_2$ is almost identical and not shown for clarity). The standard deviation (square root of the variance) is shown for the variances and their bounds. Bottom: the log-ratio of the upper bound (UB) provided by Theorem 4.1 and the true variance. The closer to 0 the better quality the UB. On the right most column, the variance of $\hat{\mathcal{I}}_2$ vanishes: $\mathcal{V}_2(\theta_i | \mathbf{x}) = 0 \leq \mathcal{V}_1(\theta_i | \mathbf{x})$. Therefore related curves of $\hat{\mathcal{I}}_2$ are not shown.

easily approaches a nearly linear region of the loss landscape where the local optimum resides. In practice, one should estimate and examine the scale of variances — which should not be neglected as per Fig. 1 — before choosing a preferred diagonal FIM estimator for optimization and any other purposes.

6 Relationship with the “Empirical Fisher”

In some scenarios, calculating even the estimators $\hat{\mathcal{I}}_1(\boldsymbol{\theta})$ and $\hat{\mathcal{I}}_2(\boldsymbol{\theta})$ of the diagonal FIM can still be expensive. Part of this cost comes from requiring label samples \mathbf{y}_k for each \mathbf{x}_k and their associated backward passes, Eqs. (3) and (4). For instance, when the FIM is used in an iterative optimization procedure, \mathbf{y}_k need to be re-sampled at each learning step w.r.t. the current \mathbf{h} and additional backpropagation needs to be run for each k .

As such, different ‘FIM-like’ objects have been explored which replace the samples from $p(\mathbf{y} | \mathbf{x})$ with samples taken from an underlying true (but unknown) data distribution $q(\mathbf{y} | \mathbf{x})$ (Le Roux et al., 2007; Martens et al., 2010), *i.e.* utilizing samples from the data directly. We define the data’s joint distribution as $q(\mathbf{x}, \mathbf{y}) := q(\mathbf{x})q(\mathbf{y} | \mathbf{x})$. In analogy to the FIM, the *data Fisher information matrix* (DFIM) can be defined as the PSD tensor $\mathbf{I}(\boldsymbol{\theta}) := \mathbb{E}_{q(\mathbf{x})}[\mathbf{I}(\boldsymbol{\theta} | \mathbf{x})]$, with

$$\mathbf{I}(\boldsymbol{\theta} | \mathbf{x}) = \mathbb{E}_{q(\hat{\mathbf{y}} | \mathbf{x})} \left[\frac{\partial \log p(\hat{\mathbf{y}} | \mathbf{x})}{\partial \boldsymbol{\theta}} \frac{\partial \log p(\hat{\mathbf{y}} | \mathbf{x})}{\partial \boldsymbol{\theta}^\top} \right] = \left(\frac{\partial \mathbf{h}}{\partial \boldsymbol{\theta}} \right)^\top \mathbf{I}(\mathbf{h} | \mathbf{x}) \left(\frac{\partial \mathbf{h}}{\partial \boldsymbol{\theta}} \right), \quad (21)$$

where $\mathbf{I}(\mathbf{h} | \mathbf{x}) = \mathbb{E}_{q(\hat{\mathbf{y}} | \mathbf{x})} [(\mathbf{t}(\hat{\mathbf{y}}) - \boldsymbol{\eta}(\mathbf{x}))(\mathbf{t}(\hat{\mathbf{y}}) - \boldsymbol{\eta}(\mathbf{x}))^\top]$ denotes the 2nd (non-central) moment of $(\mathbf{t}(\hat{\mathbf{y}}) - \boldsymbol{\eta}(\mathbf{x}))$ w.r.t. $q(\hat{\mathbf{y}} | \mathbf{x})$, and $\partial \mathbf{h} / \partial \boldsymbol{\theta}$ is the Jacobian of the map $\boldsymbol{\theta} \rightarrow \mathbf{h}$. In the special case that $q(\mathbf{y} | \mathbf{x}) = p(\mathbf{y} | \mathbf{x}, \boldsymbol{\theta})$, then $\mathbf{I}(\boldsymbol{\theta} | \mathbf{x})$ becomes exactly $\mathcal{I}(\boldsymbol{\theta} | \mathbf{x})$.

The DFIM $\mathbf{I}(\boldsymbol{\theta} | \mathbf{x})$ in Eq. (21) is a more general definition. Compared to the FIM $\mathcal{I}(\boldsymbol{\theta} | \mathbf{x})$, it yields a different PSD tensor on $\boldsymbol{\theta}$ parameter space (the neuromanifold) depending on a distribution $q(\mathbf{x}, \mathbf{y})$, which is neither necessarily on the same neuromanifold nor necessarily parametric at all. Indeed, an asymmetry in the true data distribution and the empirical one induces a different geometric structure (Critchley et al., 1993). By definition, we have

$$\mathbf{I}(\boldsymbol{\theta} | \mathbf{x}) \succeq \left(\frac{\partial \text{KL}}{\partial \boldsymbol{\theta}} \right) \left(\frac{\partial \text{KL}}{\partial \boldsymbol{\theta}} \right)^\top,$$

where $\text{KL}(\boldsymbol{\theta}) := \int q(\hat{\mathbf{y}} | \mathbf{x}) \log \frac{q(\hat{\mathbf{y}} | \mathbf{x})}{p(\hat{\mathbf{y}} | \mathbf{x}, \boldsymbol{\theta})} d\hat{\mathbf{y}}$ is the Kullback-Leibler (KL) divergence, or the loss to be minimized. The DFIM can be regarded as a surrogate function of the squared gradient of the KL divergence. It is a symmetric covariant tensor and satisfies the same rule w.r.t. reparameterization as the FIM. Consider the reparameterization $\boldsymbol{\theta} \rightarrow \boldsymbol{\zeta}$, the DFIM becomes $\mathbf{I}(\boldsymbol{\zeta} | \mathbf{x}) = (\partial \boldsymbol{\theta} / \partial \boldsymbol{\zeta})^\top \mathbf{I}(\boldsymbol{\theta} | \mathbf{x}) (\partial \boldsymbol{\theta} / \partial \boldsymbol{\zeta})$.

Notice that $\hat{\boldsymbol{\eta}}(\mathbf{x}) := \mathbb{E}_{q(\hat{\mathbf{y}} | \mathbf{x})}[\mathbf{t}(\hat{\mathbf{y}})] \neq \boldsymbol{\eta}(\mathbf{x})$ in general. As such, there will be a miss-match when utilizing $\mathbf{I}(\mathbf{h} | \mathbf{x})$ as a substitute for $\mathcal{I}(\mathbf{h} | \mathbf{x})$. However, as learning progresses and $p(\hat{\mathbf{y}} | \mathbf{x})$ becomes more similar to the data’s true labeling posterior $q(\hat{\mathbf{y}} | \mathbf{x})$, the DFIM will become closer to the FIM.

If $q(\mathbf{x}, \mathbf{y}) = \frac{1}{N} \sum_{k=1}^N \delta(\mathbf{x} - \mathbf{x}_k) \cdot \delta(\mathbf{y} - \mathbf{y}_k)$ is defined by the observed samples, DFIM gives the widely used “*Empirical Fisher*” (Martens, 2020), whose diagonal entries are

$$\hat{\mathbf{I}}(\theta_i) = \frac{1}{N} \sum_{k=1}^N (\partial \mathbf{h}_i^a(\mathbf{x}_k) \cdot (\mathbf{t}_a(\hat{\mathbf{y}}_k) - \boldsymbol{\eta}_a(\mathbf{x}_k)))^2,$$

where $(\mathbf{x}_1, \hat{\mathbf{y}}_1), \dots, (\mathbf{x}_N, \hat{\mathbf{y}}_N)$ are i.i.d. sampled from $q(\mathbf{x}, \hat{\mathbf{y}})$. Similarly to $\hat{\mathcal{I}}_1(\theta_i)$, an estimator with a fixed input \mathbf{x} can be considered, denoted as $\hat{\mathbf{I}}(\theta_i | \mathbf{x})$.

Given the computational benefits of being able to use data directly (and not require a separate sampling routine), many popular optimization methods utilize (an approximation of) the empirical Fisher.

For instance, in the Adam optimizer (Kingma & Ba, 2015), the empirical Fisher is used to obtain an approximation of the diagonal FIM and to adapt to the geometry of the data. However, the change of switching from samples \mathbf{y}_k to $\hat{\mathbf{y}}_k$ is anything but superficial (Martens, 2020, Chapter 11) — $\hat{\mathcal{I}}(\boldsymbol{\theta})$ is *not* an unbiased estimator of $\mathcal{I}(\boldsymbol{\theta})$ as $\mathcal{I}(\mathbf{h} | \mathbf{x})$ is different from $\mathcal{I}(\mathbf{h} | \mathbf{x})$.

The biased nature of the empirical Fisher affects the other moments of the estimator as well. In particular, we do not have the same equivalence of covariance and the metric being pulled back by $\boldsymbol{\theta} \rightarrow \mathbf{h}$ (Sun, 2020).

Lemma 6.1. *Given the conditional data distribution $q(\hat{\mathbf{y}} | \mathbf{x})$, the covariance of \mathbf{t} given \mathbf{x} is given by*

$$\text{Cov}^q(\mathbf{t} | \mathbf{x}) = \mathcal{I}(\mathbf{h} | \mathbf{x}) - \Delta\mathcal{H}(\mathbf{x}), \quad (22)$$

where $\Delta\mathcal{H}(\mathbf{x}) = (\boldsymbol{\eta}(\mathbf{x}) - \hat{\boldsymbol{\eta}}(\mathbf{x}))(\boldsymbol{\eta}(\mathbf{x}) - \hat{\boldsymbol{\eta}}(\mathbf{x}))^\top$.

As a result, although the estimator $\hat{\mathcal{I}}(\theta_i | \mathbf{x})$ emits a similar form to $\mathcal{V}_1(\theta_i | \mathbf{x})$ (i.e., Eq. (11)), the bounds are expressed via non-central moments of $(\mathbf{t}(\hat{\mathbf{y}}) - \boldsymbol{\eta}(\mathbf{x}))$ and not the central moments of \mathbf{t} which were used in the estimators of the FIM — noting the miss-match in $\hat{\boldsymbol{\eta}}(\mathbf{x}) \neq \boldsymbol{\eta}(\mathbf{x})$. Some corresponding DFIM bounds are characterized in Appendix F.

7 Conclusion

We have analyzed two different estimators $\hat{\mathcal{I}}_1(\boldsymbol{\theta})$ and $\hat{\mathcal{I}}_2(\boldsymbol{\theta})$ for the diagonal entries of the FIM. The variances of these estimators are determined by both the non-linearity of the neural network and the moments of the exponential family. We find distinct scenarios where each estimator is preferable through empirically examining the estimator variances and bounds. We connect the investigated estimators with the empirical Fisher. Future directions include to extend the analysis to the FIM block diagonals (e.g. Martens & Grosse (2015); Ren & Goldfarb (2021)) and to adapt the current NN optimizers (e.g. Kingma & Ba (2015)) to consider the FIM variances.

8 Acknowledgements

The authors thank Frank Nielsen for their insightful feedback.

References

- Amari, S. *Information Geometry and Its Applications*, volume 194 of *Applied Mathematical Sciences*. Springer-Verlag, Berlin, 2016.
- Amari, S., Ozeki, T., Karakida, R., Yoshida, Y., and Okada, M. Dynamics of learning in MLP: Natural gradient and singularity revisited. *Neural Computation*, 30(1):1–33, 2018.
- Amari, S., Karakida, R., and Oizumi, M. Fisher information and natural gradient learning in random deep networks. In *International Conference on Artificial Intelligence and Statistics*, pp. 694–702. PMLR, 2019.
- Becker, S., Le Cun, Y., et al. Improving the convergence of back-propagation learning with second order methods. In *Proceedings of the 1988 connectionist models summer school*, pp. 29–37, 1988.
- Critchley, F., Marriott, P., and Salmon, M. Preferred point geometry and statistical manifolds. *The Annals of Statistics*, pp. 1197–1224, 1993.

- Dangel, F., Kunstner, F., and Hennig, P. Backpack: Packing more into backprop. *arXiv preprint arXiv:1912.10985*, 2019.
- Deng, L. The MNIST database of handwritten digit images for machine learning research. *IEEE Signal Processing Magazine*, 29(6):141–142, 2012.
- Efron, B. Curvature and inference for maximum likelihood estimates. *The Annals of Statistics*, 46(4): 1664–1692, 2018.
- Elsayed, M. and Mahmood, A. R. Hessscale: Scalable computation of Hessian diagonals. *arXiv preprint arXiv:2210.11639*, 2022.
- Feinman, R. Pytorch-minimize: a library for numerical optimization with autograd, 2021. URL <https://github.com/rfeinman/pytorch-minimize>.
- Foret, P., Kleiner, A., Mobahi, H., and Neyshabur, B. Sharpness-aware minimization for efficiently improving generalization. *arXiv preprint arXiv:2010.01412*, 2020.
- Guo, S. and Spall, J. C. Relative accuracy of two methods for approximating observed Fisher information. In *Data-Driven Modeling, Filtering and Control: Methods and applications*, pp. 189–211. IET Press, London, 2019.
- Heskes, T. On “natural” learning and pruning in multilayered perceptrons. *Neural Computation*, 12(4): 881–901, 2000.
- Karakida, R. and Osawa, K. Understanding approximate fisher information for fast convergence of natural gradient descent in wide neural networks. *Advances in neural information processing systems*, 33: 10891–10901, 2020.
- Karakida, R., Akaho, S., and Amari, S. Universal statistics of Fisher information in deep neural networks: Mean field approach. In *International Conference on Artificial Intelligence and Statistics*, pp. 1032–1041. PMLR, 2019.
- Karakida, R., Akaho, S., and Amari, S.-i. Pathological spectra of the Fisher information metric and its variants in deep neural networks. *Neural Computation*, 33(8):2274–2307, 2021.
- Kingma, D. P. and Ba, J. Adam: A method for stochastic optimization. In *International Conference on Learning Representations*, 2015.
- Kolda, T. G. and Mayo, J. R. An adaptive shifted power method for computing generalized tensor eigenpairs. *SIAM Journal on Matrix Analysis and Applications*, 35(4):1563–1581, 2014.
- Kunstner, F., Balles, L., and Hennig, P. Limitations of the empirical Fisher approximation for natural gradient descent. In *Advances in Neural Information Processing Systems*, pp. 4133–4144. Curran Associates, Inc., 2020.
- Kurita, T. Iterative weighted least squares algorithms for neural networks classifiers. *New generation computing*, 12:375–394, 1994.
- Le Roux, N., Manzagol, P.-A., and Bengio, Y. Topmoumoute online natural gradient algorithm. *Advances in neural information processing systems*, 20, 2007.
- Li, H., Xu, Z., Taylor, G., Studer, C., and Goldstein, T. Visualizing the loss landscape of neural nets. *Advances in neural information processing systems*, 31, 2018.

- Lim, L.-H. Singular values and eigenvalues of tensors: a variational approach. In *1st IEEE International Workshop on Computational Advances in Multi-Sensor Adaptive Processing, 2005.*, pp. 129–132. IEEE, 2005.
- Marshall, A. W., Olkin, I., and Arnold, B. C. *Inequalities: Theory of Majorization and its Applications*, volume 143. Springer, second edition, 2011. doi: 10.1007/978-0-387-68276-1.
- Martens, J. New insights and perspectives on the natural gradient method. *Journal of Machine Learning Research*, 21(146):1–76, 2020.
- Martens, J. and Grosse, R. Optimizing neural networks with Kronecker-factored approximate curvature. In *International Conference on Machine Learning*, pp. 2408–2417. PMLR, 2015.
- Martens, J. et al. Deep learning via Hessian-free optimization. In *ICML*, volume 27, pp. 735–742, 2010.
- Nickl, P., Xu, L., Taylor, D., Möllenhoff, T., and Khan, M. E. E. The memory-perturbation equation: Understanding model’s sensitivity to data. In *Advances in Neural Information Processing Systems*, volume 36, pp. 26923–26949. Curran Associates, Inc., 2023.
- Nielsen, F. and Hadjeres, G. *Monte Carlo Information-Geometric Structures*, pp. 69–103. Springer International Publishing, 2019.
- Ollivier, Y. Riemannian metrics for neural networks I: feedforward networks. *Information and Inference: A Journal of the IMA*, 4(2):108–153, 2015.
- Pascanu, R. and Bengio, Y. Revisiting natural gradient for deep networks. In *International Conference on Learning Representations*, 2014.
- Paszke, A., Gross, S., Massa, F., Lerer, A., Bradbury, J., Chanan, G., Killeen, T., Lin, Z., Gimelshein, N., Antiga, L., Desmaison, A., Kopf, A., Yang, E., DeVito, Z., Raison, M., Tejani, A., Chilamkurthy, S., Steiner, B., Fang, L., Bai, J., and Chintala, S. Pytorch: An imperative style, high-performance deep learning library. In *Advances in Neural Information Processing Systems*, pp. 8024–8035. Curran Associates, Inc., 2019.
- Pennington, J. and Worah, P. The spectrum of the Fisher information matrix of a single-hidden-layer neural network. In *Advances in Neural Information Processing Systems*, pp. 5415–5424, 2018.
- Ren, Y. and Goldfarb, D. Tensor normal training for deep learning models. In *Advances in Neural Information Processing Systems*, volume 34, pp. 26040–26052. Curran Associates, Inc., 2021.
- Soen, A. and Sun, K. On the variance of the Fisher information for deep learning. In *Advances in Neural Information Processing Systems*, 2021.
- Sun, K. Information geometry for data geometry through pullbacks. In *Deep Learning through Information Geometry (Workshop at NeurIPS 2020)*, 2020.
- Sun, K. and Nielsen, F. Relative Fisher information and natural gradient for learning large modular models. In *International Conference on Machine Learning*, pp. 3289–3298. PMLR, 2017.
- Sun, K. and Nielsen, F. A geometric modeling of Occam’s razor in deep learning. *arXiv preprint arXiv:1905.11027*, 2019.
- Tao, T. *Topics in random matrix theory*, volume 132. American Mathematical Soc., 2012.
- Wang, S.-D., Kuo, T.-S., and Hsu, C.-F. Trace bounds on the solution of the algebraic matrix riccati and lyapunov equation. *IEEE Transactions on Automatic Control*, 31(7):654–656, 1986.

- Withers, C. S. and Nadarajah, S. The spectral decomposition and inverse of multinomial and negative multinomial covariances. *Brazilian Journal of Probability and Statistics*, pp. 376–380, 2014.
- Yao, Z., Gholami, A., Keutzer, K., and Mahoney, M. W. Pyhessian: Neural networks through the lens of the Hessian. In *2020 IEEE international conference on big data (Big data)*, pp. 581–590. IEEE, 2020.
- Yao, Z., Gholami, A., Shen, S., Mustafa, M., Keutzer, K., and Mahoney, M. Adahessian: An adaptive second order optimizer for machine learning. In *proceedings of the AAAI conference on artificial intelligence*, volume 35, pp. 10665–10673, 2021.

Supplementary Material

Abstract

This is the Supplementary Material to Paper "Tradeoffs of Diagonal Fisher Information Matrix Estimators". To differentiate with the numberings in the main file, the numbering of Theorems is letter-based (A, B, ...).

Table of Contents

Additional Results

⇒ Appendix A: The Conditional Variances in Closed Form	Pg 17
⇒ Appendix B: Off-Diagonal Variance	Pg 17
⇒ Appendix C: Bounding the Trace Variance by Full Spectrum	Pg 18
⇒ Appendix D: Second Central Moment of Categorical Distribution	Pg 21
⇒ Appendix E: Empirical Results Continued	Pg 21
⇒ Appendix F: "Empirical Fisher" Continued	Pg 22

Proof

⇒ Appendix G: Derivation of Eqs. (5) and (6)	Pg 23
⇒ Appendix H: Proof of Eq. (10)	Pg 24
⇒ Appendix I: Proof of Eq. (11)	Pg 25
⇒ Appendix J: Proof of Eq. (12)	Pg 26
⇒ Appendix K: Proof of Corollary 4.2	Pg 26
⇒ Appendix L: Proof of Proposition 4.3	Pg 28
⇒ Appendix M: Proof of Corollary 4.6	Pg 28
⇒ Appendix N: Proof of Theorem 4.7	Pg 30
⇒ Appendix O: Proof of Lemma 4.8	Pg 33
⇒ Appendix P: Proof of Proposition 5.1	Pg 33
⇒ Appendix Q: Proof of Theorem 5.2	Pg 34
⇒ Appendix R: Proof of Lemma 6.1	Pg 35
⇒ Appendix S: Proof of Corollary F.1	Pg 35
⇒ Appendix T: Proof of Corollary F.2	Pg 36

A The Conditional Variances in Closed Form

We consider the diagonal entries of the conditional FIM $\mathcal{I}(\theta_i | \mathbf{x})$ and the conditional variances $\mathcal{V}_j(\theta_i | \mathbf{x})$ of its estimators in closed form.

Lemma A.1. $\forall \mathbf{x} \in \mathbb{R}^I, \forall i = 1, \dots, \dim(\boldsymbol{\theta}),$

$$\mathcal{I}(\theta_i | \mathbf{x}) = \partial_i \mathbf{h}^a(\mathbf{x}) \partial_i \mathbf{h}^b(\mathbf{x}) \mathcal{I}_{ab}(\mathbf{h} | \mathbf{x}), \quad (23)$$

$$\mathcal{V}_1(\theta_i | \mathbf{x}) = \frac{1}{N} \partial_i \mathbf{h}^a(\mathbf{x}) \partial_i \mathbf{h}^b(\mathbf{x}) \partial_i \mathbf{h}^c(\mathbf{x}) \partial_i \mathbf{h}^d(\mathbf{x}) \cdot [\mathcal{K}_{abcd}^p(\mathbf{t} | \mathbf{x}) - \mathcal{I}_{ab}(\mathbf{h} | \mathbf{x}) \cdot \mathcal{I}_{cd}(\mathbf{h} | \mathbf{x})], \quad (24)$$

$$\mathcal{V}_2(\theta_i | \mathbf{x}) = \frac{1}{N} \partial_{ii}^2 \mathbf{h}^a(\mathbf{x}) \partial_{ii}^2 \mathbf{h}^b(\mathbf{x}) \mathcal{I}_{ab}(\mathbf{h} | \mathbf{x}), \quad (25)$$

where $\partial_i \mathbf{h}(\mathbf{x}) := \partial \mathbf{h}(\mathbf{x}) / \partial \theta_i$; $\partial_{ij} \mathbf{h}(\mathbf{x}) := \partial^2 \mathbf{h}(\mathbf{x}) / \partial \theta_i \partial \theta_j$;

Proof. The proof directly follows from [Soen & Sun \(2021, Equation 6\)](#), [Soen & Sun \(2021, Theorem 4\)](#), and [Soen & Sun \(2021, Theorem 6\)](#) \square

Lemma A.1 shows that, for the former, $\mathcal{V}_1(\theta_i | \mathbf{x})$ only depends on 1st order derivatives; while $\mathcal{V}_2(\theta_i | \mathbf{x})$ only depends on the 2nd order derivatives. For the latter, $\mathcal{V}_1(\theta_i | \mathbf{x})$ depends on both the 2nd and 4th central moments of $\mathbf{t}(\mathbf{y})$; while $\mathcal{V}_2(\theta_i | \mathbf{x})$ only depends on the 2nd central moments.

Given $\mathcal{I}_{ab}(\mathbf{h} | \mathbf{x})$ and $\partial_i \mathbf{h}^a(\mathbf{x})$, the computational complexity of all diagonal entries $\mathcal{I}(\theta_i | \mathbf{x})$ is $\mathcal{O}(T^2 \dim(\boldsymbol{\theta}))$. If $\mathcal{K}_{abcd}^p(\mathbf{t} | \mathbf{x})$ and $\partial_{ii}^2 \mathbf{h}^a(\mathbf{x})$ are given, then the computational complexity of the variances in Eqs. (24) and (25) is respectively $\mathcal{O}(T^4 \dim(\boldsymbol{\theta}))$ and $\mathcal{O}(T^2 \dim(\boldsymbol{\theta}))$. Each requires to evaluate a $T \times \dim(\boldsymbol{\theta})$ matrix, either $\partial_i \mathbf{h}^a(\mathbf{x})$ or $\partial_{ii}^2 \mathbf{h}^a(\mathbf{x})$ — which can be expensive to calculate for the latter. This is why we need efficient estimators and / or bounds for the tensors on the LHS of Eqs. (23) to (25).

B Off-Diagonal Variance

We consider an off-diagonal version of the bound given by [Theorem 4.1](#). Notice that in terms of the dependence on neural network weights, the only change is splitting the “responsibility” of the i th and j th parameter norms.

Theorem B.1. $\forall \mathbf{x} \in \mathbb{R}^I,$

$$\text{Var} \left(\hat{\mathcal{I}}_1(\boldsymbol{\theta} | \mathbf{x})_{ij} \right) \leq \frac{1}{N} \cdot \|\partial_i \mathbf{h}(\mathbf{x})\|_2^2 \cdot \|\partial_j \mathbf{h}(\mathbf{x})\|_2^2 \cdot \tilde{\gamma}_{\max}(\mathcal{M}), \quad (26)$$

$$\text{Var} \left(\hat{\mathcal{I}}_2(\boldsymbol{\theta} | \mathbf{x})_{ij} \right) \leq \frac{1}{N} \cdot \|\partial_{ij}^2 \mathbf{h}(\mathbf{x})\|_2^2 \cdot \gamma_{\max}(\mathcal{I}(\mathbf{h} | \mathbf{x})), \quad (27)$$

where

$$\begin{aligned} \tilde{\gamma}_{\max}(\mathcal{M}) &= \sup_{\mathbf{u}: \|\mathbf{u}\|_2=1, \mathbf{v}: \|\mathbf{v}\|_2=1} \mathbf{u}^a \mathbf{v}^b \mathbf{u}^c \mathbf{v}^d \mathcal{M}_{abcd} \\ \gamma_{\max}(M) &= \sup_{\mathbf{u}: \|\mathbf{u}\|_2=1, \mathbf{v}: \|\mathbf{v}\|_2=1} \mathbf{u}^a \mathbf{v}^b M_{ab}. \end{aligned}$$

Proof. The proof follows similarly to [Appendices I and J](#), where the primary difference is just swapping the regular eigenvalue-like quantities with the γ variational forms. \square

It should be noted that the corresponding lower bounds become trivial as the additional degree of freedom of having an inf over both \mathbf{u} and \mathbf{v} causes the corresponding γ_{\min} definition to have negative quantities. Although it is unclear what the “tensor-like” variational quantity $\tilde{\gamma}_{\max}(\mathcal{M})$ will be, for a matrix, we have the following equivalence.

Lemma B.2. $\gamma_{\max}(A) = s_{\max}(A)$, where $s_{\max}(A)$ is the maximum singular value of A .

Proof. The proof follows from optimizing over \mathbf{u} and \mathbf{v} separately:

$$\begin{aligned}\gamma_{\max}(A) &= \sup_{\mathbf{u}: \|\mathbf{u}\|_2=1} \sup_{\mathbf{v}: \|\mathbf{v}\|_2=1} \mathbf{u}^a \mathbf{v}^b A_{ab} \\ &= \sup_{\mathbf{u}: \|\mathbf{u}\|_2=1} \sup_{\mathbf{v}: \|\mathbf{v}\|_2=1} \mathbf{u}^\top A \mathbf{v} \\ &= \sup_{\mathbf{v}: \|\mathbf{v}\|_2=1} \frac{(\mathbf{A}\mathbf{v})^\top \mathbf{A}\mathbf{v}}{\|\mathbf{A}\mathbf{v}\|_2} \\ &= \sup_{\mathbf{v}: \|\mathbf{v}\|_2=1} \sqrt{\mathbf{v}^\top (A^\top A) \mathbf{v}}.\end{aligned}$$

This is equivalent to the square root of the maximal eigenvalue of $A^\top A$, which is exactly the maximum singular value. \square

Hence for the $\hat{\mathcal{I}}_2$ we have the following.

Corollary B.3. $\forall \mathbf{x} \in \mathbb{R}^I$,

$$\text{Var}\left(\hat{\mathcal{I}}_2(\boldsymbol{\theta} | \mathbf{x})_{ij}\right) \leq \frac{1}{N} \cdot \|\partial_{ij}^2 \mathbf{h}(\mathbf{x})\|_2^2 \cdot s_{\max}(\mathcal{I}(\mathbf{h} | \mathbf{x})). \quad (28)$$

C Bounding the Trace Variance by Full Spectrum

Theorem C.1. For any $\mathbf{x} \in \mathbb{R}^I$,

$$\begin{aligned}\sum_{t=1}^T s_t^2(\partial \mathbf{h}(\mathbf{x})) \cdot \lambda_{T-t+1}(\mathcal{I}(\mathbf{h} | \mathbf{x})) &\leq \text{tr}(\mathcal{I}(\boldsymbol{\theta} | \mathbf{x})) \\ &\leq \sum_{t=1}^T s_t^2(\partial \mathbf{h}(\mathbf{x})) \cdot \lambda_t(\mathcal{I}(\mathbf{h} | \mathbf{x})),\end{aligned} \quad (29)$$

$$\begin{aligned}\frac{1}{N} \cdot \sum_{t=1}^T s_t^2(\text{vJac}(\mathbf{h} | \mathbf{x})) \cdot \lambda_{T-t+1}(\overline{\mathcal{M}}) &\leq \mathcal{V}_1(\boldsymbol{\theta} | \mathbf{x}) \\ \frac{1}{N} \cdot \sum_{t=1}^T s_t^2(\text{vJac}(\mathbf{h} | \mathbf{x})) \cdot \lambda_t(\overline{\mathcal{M}}),\end{aligned} \quad (30)$$

$$\begin{aligned}\frac{1}{N} \cdot \sum_{t=1}^T s_t^2(\text{dHes}(\mathbf{h} | \mathbf{x})) \cdot \lambda_{T-t+1}(\mathcal{I}(\mathbf{h} | \mathbf{x})) &\leq \mathcal{V}_2(\boldsymbol{\theta} | \mathbf{x}) \\ &\leq \frac{1}{N} \cdot \sum_{t=1}^T s_t^2(\text{dHes}(\mathbf{h} | \mathbf{x})) \cdot \lambda_t(\mathcal{I}(\mathbf{h} | \mathbf{x})),\end{aligned} \quad (31)$$

where $s_i^2(A) = \lambda_i(A^\top A)$ denotes the i -th singular values, $\overline{\mathcal{M}}$ is the “reshaped” matrix of \mathcal{M} defined in Theorem 4.1 — i.e. there exists j, k such that $\overline{\mathcal{M}}_{jk} = \mathcal{M}_{abcd}$ for all a, b, c, d ,

$$\text{dHes}(\mathbf{h} | \mathbf{x}) = (\text{diag}(\text{Hes}(\mathbf{h}_1 | \mathbf{x})), \dots, \text{diag}(\text{Hes}(\mathbf{h}_T | \mathbf{x}))),$$

and

$$\text{vJac}(\mathbf{h} | \mathbf{x}) = (\text{vec}(\partial_1 \mathbf{h}(\mathbf{x}) \partial_1 \mathbf{h}(\mathbf{x})^\top), \dots, \text{vec}(\partial_T \mathbf{h}(\mathbf{x}) \partial_T \mathbf{h}(\mathbf{x})^\top)).$$

Proof. The proof follows from a generalized Ruhe’s trace inequality (Marshall et al., 2011):

Theorem C.2. For $A, B \in \mathfrak{R}^{n \times n}$ Hermitian matrices, we have that

$$\sum_{i=1}^n \lambda_i(A) \cdot \lambda_{n-i+1}(B) \leq \text{tr}(AB) \leq \sum_{i=1}^n \lambda_i(A) \cdot \lambda_i(B).$$

We prove the result for each equations.

For readability, we let $J^{ia} = \partial_i \mathbf{h}^a(\mathbf{x})$.

For Eq. (29):

One can notice that the trace of the FIM can exactly be expressed as the trace of two matrices.

$$\begin{aligned} \text{tr}(\mathcal{I}(\boldsymbol{\theta} | \mathbf{x})) &= \sum_{i=1}^{\dim(\boldsymbol{\theta})} \partial_i \mathbf{h}^a(\mathbf{x}) \partial_i \mathbf{h}^b(\mathbf{x}) \mathcal{I}_{ab}(\mathbf{h} | \mathbf{x}) \\ &= \mathcal{I}_{ab}(\mathbf{h} | \mathbf{x}) \sum_{i=1}^{\dim(\boldsymbol{\theta})} J^{ia} J^{ib} \\ &= \mathcal{I}_{ab}(\mathbf{h} | \mathbf{x}) \sum_{i=1}^{\dim(\boldsymbol{\theta})} (J^\top)^{ai} J^{ib} \\ &= \mathcal{I}_{ab}(\mathbf{h} | \mathbf{x}) (J^\top J)^{ab} \\ &= \text{tr}((J^\top J) \mathcal{I}(\mathbf{h} | \mathbf{x})). \end{aligned}$$

Thus, noting that the eigenvalue of the “squared” matrix is the matrix’s singular value $\lambda_t(J^\top J) = s_t^2(J)$, with Theorem C.2, we have that:

$$\sum_{t=1}^T s_t^2(\partial \mathbf{h}(\mathbf{x})) \cdot \lambda_{T-t+1}(\mathcal{I}(\mathbf{h} | \mathbf{x})) \leq \text{tr}(\mathcal{I}(\boldsymbol{\theta} | \mathbf{x})) \leq \sum_{t=1}^T s_t^2(\partial \mathbf{h}(\mathbf{x})) \cdot \lambda_t(\mathcal{I}(\mathbf{h} | \mathbf{x})).$$

For Eq. (30):

Noting that $\mathcal{M}_{abcd} = \mathcal{K}_{abcd}^p(\mathbf{t} | \mathbf{x}) - \mathcal{I}_{ab}(\mathbf{h} | \mathbf{x}) \cdot \mathcal{I}_{cd}(\mathbf{h} | \mathbf{x})$. Furthermore, we have that

$$\text{vJac}(\mathbf{h} | \mathbf{x}) = (\text{vec}(\partial_1 \mathbf{h}(\mathbf{x}) \partial_1 \mathbf{h}(\mathbf{x})^\top), \dots, \text{vec}(\partial_T \mathbf{h}(\mathbf{x}) \partial_T \mathbf{h}(\mathbf{x})^\top)).$$

Let us define the following 3D tensor with $\mathcal{J}^{iab} = \partial_i \mathbf{h}^a(\mathbf{x}) \partial_i \mathbf{h}^b(\mathbf{x}) = (\partial_i \mathbf{h}(\mathbf{x}) \partial_i^\top \mathbf{h}(\mathbf{x}))^{ab}$.

$$\begin{aligned}
\mathcal{V}_1(\boldsymbol{\theta} | \mathbf{x}) &= \frac{1}{N} \sum_{i=1}^{\dim(\boldsymbol{\theta})} \partial_i \mathbf{h}^a(\mathbf{x}) \partial_i \mathbf{h}^b(\mathbf{x}) \partial_i \mathbf{h}^c(\mathbf{x}) \partial_i \mathbf{h}^d(\mathbf{x}) \mathcal{M}_{abcd} \\
&= \frac{1}{N} \mathcal{M}_{abcd} \sum_{i=1}^{\dim(\boldsymbol{\theta})} \mathcal{J}^{iab} \mathcal{J}^{icd} \\
&= \frac{1}{N} \sum_{a,b=1}^T \sum_{c,d=1}^T \mathcal{M}_{abcd} \sum_{i=1}^{\dim(\boldsymbol{\theta})} \mathcal{J}^{iab} \mathcal{J}^{icd} \\
&= \frac{1}{N} \sum_{j=1}^{T^2} \sum_{k=1}^{T^2} \overline{\mathcal{M}}_{jk} \sum_{i=1}^{\dim(\boldsymbol{\theta})} \text{vJac}^{ij}(\mathbf{h} | \mathbf{x}) \text{vJac}^{ik}(\mathbf{h} | \mathbf{x}) \\
&= \frac{1}{N} \sum_{j=1}^{T^2} \sum_{k=1}^{T^2} \overline{\mathcal{M}}_{jk} (\text{vJac}^\top(\mathbf{h} | \mathbf{x}) \text{vJac}(\mathbf{h} | \mathbf{x}))^{jk} \\
&= \frac{1}{N} \text{tr} \left(\overline{\mathcal{M}} (\text{vJac}^\top(\mathbf{h} | \mathbf{x}) \text{vJac}(\mathbf{h} | \mathbf{x})) \right).
\end{aligned}$$

Thus, again simplifying the eigenvalue of the ‘‘squared’’ matrix, with Theorem C.2, we have that:

$$\frac{1}{N} \sum_{t=1}^T s_t^2(\text{vJac}(\mathbf{h} | \mathbf{x})) \cdot \lambda_{T-t+1}(\overline{\mathcal{M}}) \leq \text{tr} \left(\hat{\mathcal{I}}_1(\boldsymbol{\theta} | \mathbf{x}) \right) \leq \frac{1}{N} \sum_{t=1}^T s_t^2(\text{vJac}(\mathbf{h} | \mathbf{x})) \cdot \lambda_t(\overline{\mathcal{M}}).$$

For Eq. (31):

Similar to Eq. (29), we only need to rearrange the summation. Notice that

$$\text{dHes}(\mathbf{h} | \mathbf{x}) = (\text{diag}(\text{Hes}(\mathbf{h}_1 | \mathbf{x})), \dots, \text{diag}(\text{Hes}(\mathbf{h}_T | \mathbf{x}))),$$

thus $\text{dHes}^{ia}(\mathbf{h} | \mathbf{x}) = \partial_{ii}^2(\mathbf{h}_a | \mathbf{x})$.

$$\begin{aligned}
\mathcal{V}_2(\boldsymbol{\theta} | \mathbf{x}) &= \frac{1}{N} \sum_{i=1}^{\dim(\boldsymbol{\theta})} \partial_{ii}^2 \mathbf{h}^a(\mathbf{x}) \partial_{ii}^2 \mathbf{h}^b(\mathbf{x}) \mathcal{I}_{ab}(\mathbf{h} | \mathbf{x}) \\
&= \frac{1}{N} \mathcal{I}_{ab}(\mathbf{h} | \mathbf{x}) \sum_{i=1}^{\dim(\boldsymbol{\theta})} \partial_{ii}^2 \mathbf{h}^a(\mathbf{x}) \partial_{ii}^2 \mathbf{h}^b(\mathbf{x}) \\
&= \frac{1}{N} \mathcal{I}_{ab}(\mathbf{h} | \mathbf{x}) \sum_{i=1}^{\dim(\boldsymbol{\theta})} \text{dHes}^{ia}(\mathbf{h} | \mathbf{x}) \text{dHes}^{ib}(\mathbf{h} | \mathbf{x}) \\
&= \frac{1}{N} \mathcal{I}_{ab}(\mathbf{h} | \mathbf{x}) \sum_{i=1}^{\dim(\boldsymbol{\theta})} (\text{dHes}^\top)^{ai}(\mathbf{h} | \mathbf{x}) \text{dHes}^{ib}(\mathbf{h} | \mathbf{x}) \\
&= \frac{1}{N} \mathcal{I}_{ab}(\mathbf{h} | \mathbf{x}) (\text{dHes}^\top(\mathbf{h} | \mathbf{x}) \text{dHes}(\mathbf{h} | \mathbf{x}))^{ab} \\
&= \frac{1}{N} \text{tr} \left(\mathcal{I}(\mathbf{h} | \mathbf{x}) (\text{dHes}^\top(\mathbf{h} | \mathbf{x}) \text{dHes}(\mathbf{h} | \mathbf{x})) \right).
\end{aligned}$$

Thus, again simplifying the eigenvalue of the “squared” matrix, with Theorem C.2, we have that:

$$\frac{1}{N} \sum_{t=1}^T s_t^2 (\text{dHes}(\mathbf{h} | \mathbf{x})) \cdot \lambda_{T-t+1}(\mathcal{I}(\mathbf{h} | \mathbf{x})) \leq \text{tr}(\hat{\mathcal{I}}_2(\boldsymbol{\theta} | \mathbf{x})) \leq \frac{1}{N} \sum_{t=1}^T s_t^2 (\text{dHes}(\mathbf{h} | \mathbf{x})) \cdot \lambda_t(\mathcal{I}(\mathbf{h} | \mathbf{x})).$$

□

D Second Central Moment of Categorical Distribution

Proof. We first notice that the exponential family density is given by,

$$p(y | \mathbf{x}) = \exp(\mathbf{h}_y(\mathbf{x}) - F(\mathbf{h}(\mathbf{x})))$$

and thus also have

$$F(\mathbf{h}(\mathbf{x})) = \log \sum_{t=1}^T \exp(\mathbf{h}_t(\mathbf{x}))$$

The first order derivative follows as,

$$\left. \frac{\partial F(\mathbf{h})}{\partial \mathbf{h}_i} \right|_{\mathbf{h}=\mathbf{h}(\mathbf{x})} = \frac{\exp(\mathbf{h}_i(\mathbf{x}))}{\sum_{t=1}^T \exp(\mathbf{h}_t(\mathbf{x}))} = \sigma_i(\mathbf{h}(\mathbf{x}))$$

As such, the second order derivatives also follow,

$$\begin{aligned} \left. \frac{\partial^2 F(\mathbf{h})}{\partial \mathbf{h}_i \partial \mathbf{h}_j} \right|_{\mathbf{h}=\mathbf{h}(\mathbf{x})} &= \frac{\exp(\mathbf{h}_i(\mathbf{x})) \delta_{ij} \cdot \sum_{t=1}^T \exp(\mathbf{h}_t(\mathbf{x})) - \exp(\mathbf{h}_i(\mathbf{x})) \exp(\mathbf{h}_j(\mathbf{x}))}{\left(\sum_{t=1}^T \exp(\mathbf{h}_t(\mathbf{x})) \right)^2} \\ &= \sigma_i(\mathbf{h}(\mathbf{x})) \cdot \delta_{ij} - \sigma_i(\mathbf{h}(\mathbf{x})) \sigma_j(\mathbf{h}(\mathbf{x})). \end{aligned}$$

As such, we have that

$$\mathcal{I}(\mathbf{h} | \mathbf{x}) = \text{diag}(\sigma(\mathbf{x})) - \sigma(\mathbf{x})\sigma(\mathbf{x})^\top.$$

□

E Empirical Results Continued

In the following section we present additional details and results for the experimental verification we conduct in Section 5.3.

E.1 Additional Details

We note that to calculate the diagonal Hessians required for the bounds and empirical FIM calculations, we utilize the `BackPACK` (Dangel et al., 2019) for `PyTorch`. Additionally, to calculate the sufficient statistics moment’s spectrum, we explicitly solve the minimum and maximum eigenvalues via their optimization problems. For 2D tensors / matrices, we utilize `numpy.linalg.eig`. For 4D tensors, we utilize `PyTorch Minimize` (Feinman, 2021), a wrapper for `SciPy`’s `optimize` function.

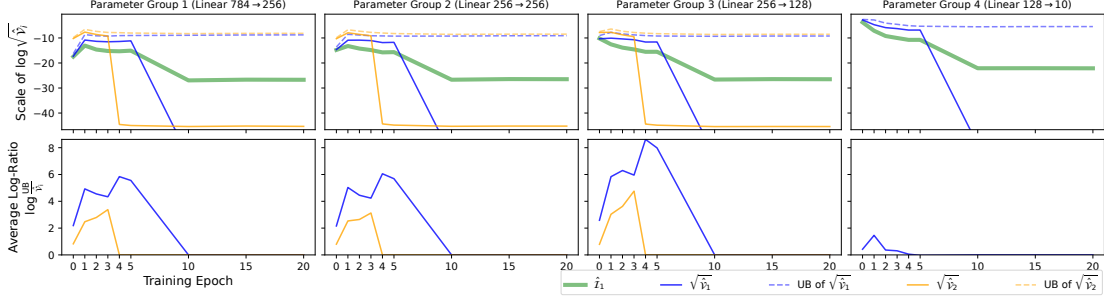


Figure I: The Fisher information, its variances and bounds of the variances w.r.t. a MLP trained with different initialization and a different input \mathbf{x} (a)

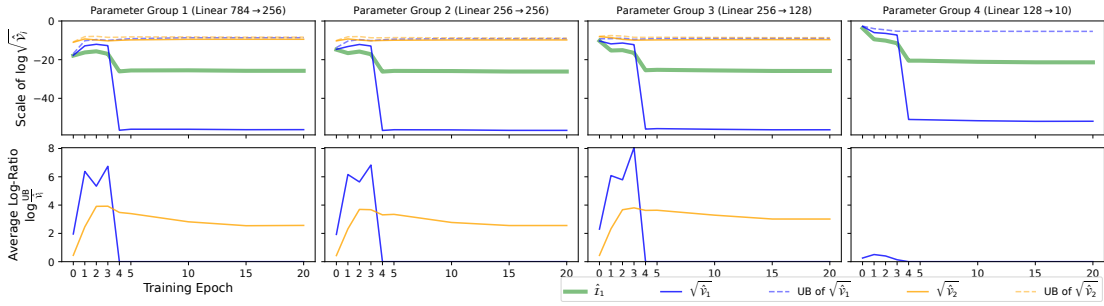


Figure II: The Fisher information, its variances and bounds of the variances w.r.t. a MLP trained with different initialization and a different input \mathbf{x} (b)

E.II Additional Plots

We present Figs. I to IV which are the exact same experiment run in Section 5.3, but with different initial NN weights and random inputs.

Figures V to IX show the experimental results on a 5-layer MLP and log-sigmoid activation function. In most of the cases, the FIM and its associated variances quickly go to zero in the first few epochs.

F “Empirical Fisher” Continued

Noting Lemma 6.1’s characterization of the covariance, we are able to characterize the variance of the diagonal elements of $\hat{\mathbf{I}}(\boldsymbol{\theta} | \mathbf{x})$, denoted as $V(\theta_i | \mathbf{x}) := \text{Var}(\hat{\mathbf{I}}(\theta_i | \mathbf{x}))$.

Corollary F.1. For any $\mathbf{x} \in \mathbb{R}^I$,

$$\begin{aligned} V(\theta_i | \mathbf{x}) &= \frac{1}{N} \partial_i \mathbf{h}^a(\mathbf{x}) \partial_i \mathbf{h}^b(\mathbf{x}) \partial_i \mathbf{h}^c(\mathbf{x}) \partial_i \mathbf{h}^d(\mathbf{x}) (\mathbf{K}_{abcd}(\mathbf{t} | \mathbf{x}) - \mathbf{I}_{ab}(\mathbf{h} | \mathbf{x}) \otimes \mathbf{I}_{cd}(\mathbf{h} | \mathbf{x})) \\ &= \frac{1}{N} \partial_i \mathbf{h}^a(\mathbf{x}) \partial_i \mathbf{h}^b(\mathbf{x}) \partial_i \mathbf{h}^c(\mathbf{x}) \partial_i \mathbf{h}^d(\mathbf{x}) \mathbf{K}_{abcd}(\mathbf{t} | \mathbf{x}) - \frac{1}{N} \left(\partial_i \mathbf{h}^\top(\mathbf{x}) (\text{Cov}^q(\mathbf{t} | \mathbf{x}) + \Delta \mathbf{H}(\mathbf{x})) \partial_i \mathbf{h}(\mathbf{x}) \right)^2, \end{aligned}$$

where $\mathbf{K}(\mathbf{h} | \mathbf{x})$ the 4th (non-central) moment of $(\mathbf{t}(\hat{\mathbf{y}}) - \boldsymbol{\eta}(\mathbf{x}))$ w.r.t. $q(\hat{\mathbf{y}} | \mathbf{x})$.

As a result of the similarity of the functional forms of the empirical Fisher $\hat{\mathbf{I}}(\boldsymbol{\theta})$ and the FIM estimator $\hat{\mathcal{I}}_1(\boldsymbol{\theta})$, it is not surprising that Corollary F.1 is similar to the variance of $\hat{\mathcal{I}}_1(\theta_i | \mathbf{x})$. Indeed, applying

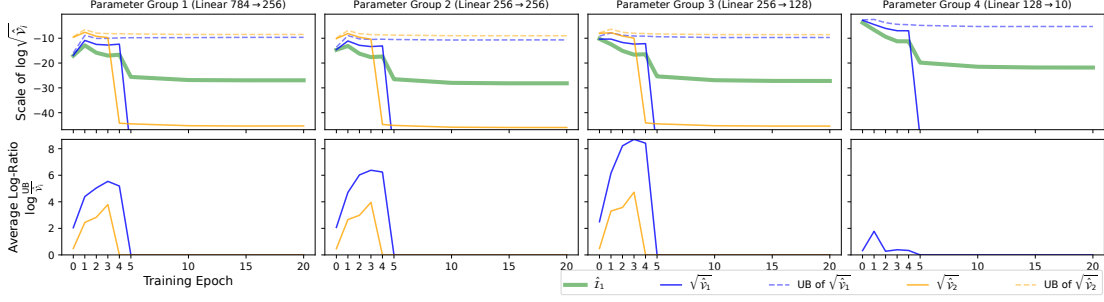


Figure III: The Fisher information, its variances and bounds of the variances w.r.t. a MLP trained with different initialization and a different input \mathbf{x} (c)

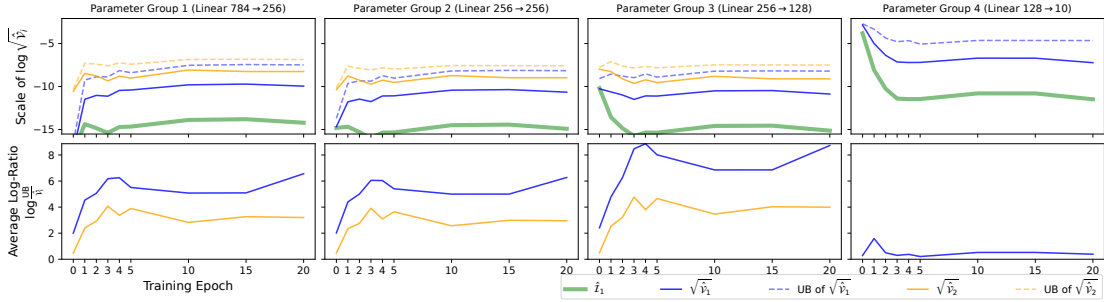


Figure IV: The Fisher information, its variances and bounds of the variances w.r.t. a MLP trained with different initialization and a different input \mathbf{x} (d)

Lemma 6.1 will give the exact same functional form with the 2nd central moments of $\mathbf{t}(\mathbf{y})$ w.r.t. $p(\mathbf{y} | \mathbf{x})$ exchanged with 2nd non-central moments of $(\mathbf{t}(\hat{\mathbf{y}}) - \boldsymbol{\eta}(\mathbf{x}))$ w.r.t. $q(\hat{\mathbf{y}} | \mathbf{x})$. $V(\theta_i | \mathbf{x})$ is therefore determined by the 2nd and the 4th moment of $(\mathbf{t}(\hat{\mathbf{y}}) - \boldsymbol{\eta}(\mathbf{x}))$ up to the parameter transformation $\boldsymbol{\theta} \rightarrow \mathbf{h}$. Subsequently, the bounds presented for $\mathcal{V}_1(\theta_i | \mathbf{x})$ (Eq. (11) and Corollary 4.6) can be similarly adapted for $V(\theta_i | \mathbf{x})$.

The extension of $V(\theta_i | \mathbf{x})$ to $V(\theta_i)$ can also be proven in a similar manner to Theorem 4.7.

Corollary F.2.

$$V(\theta_i) = \frac{1}{N} \text{Var} (I(\theta_i | \mathbf{x})) + \mathbb{E}_{q(\mathbf{x})} [V(\theta_i | \mathbf{x})], \quad (32)$$

where $\text{Var} (I(\theta_i | \mathbf{x}))$ is the variance of $I(\theta_i | \mathbf{x})$ w.r.t. $q(\mathbf{x})$.

If $q(\mathbf{x}, \mathbf{y}) = \frac{1}{N} \sum_{k=1}^N \delta(\mathbf{x} - \mathbf{x}_k) \cdot \delta(\mathbf{y} - \hat{\mathbf{y}}_k)$ for a set of observations $\{(\mathbf{x}_k, \hat{\mathbf{y}}_k)\}_{k=1}^N$, then one can directly evaluate the DFIM without sampling and achieve zero variance, i.e., $\hat{I}(\boldsymbol{\theta}) = I(\boldsymbol{\theta})$. In this scenario, there is a clear trade-off between the estimators of the FIM in Eqs. (3) and (4) and the DFIM. The estimators of the FIM are unbiased, but have a variance; while the DFIM has zero variance, but is a biased approximation of the FIM.

G Derivation of Eqs. (5) and (6)

We calculate the equations separately.

G.I Eq. (5)

Proof. For Eq. (5), we note that

$$\begin{aligned}
\frac{\partial \log p(\mathbf{y}_k | \mathbf{x}_k)}{\partial \theta_i} &= \frac{\partial}{\partial \theta_i} (\mathbf{t}^\top(\mathbf{y}_k) \mathbf{h}(\mathbf{x}_k) - F(\mathbf{h}(\mathbf{x}_k))) \\
&= \mathbf{t}_a(\mathbf{y}_k) \frac{\partial \mathbf{h}^a(\mathbf{x}_k)}{\partial \theta_i} - F'_a(\mathbf{h}(\mathbf{x}_k)) \frac{\partial \mathbf{h}^a(\mathbf{x}_k)}{\partial \theta_i} \\
&= \mathbf{t}_a(\mathbf{y}_k) \frac{\partial \mathbf{h}^a(\mathbf{x}_k)}{\partial \theta_i} - \boldsymbol{\eta}_a(\mathbf{x}_k) \frac{\partial \mathbf{h}^a(\mathbf{x}_k)}{\partial \theta_i} \\
&= (\mathbf{t}_a(\mathbf{y}_k) - \boldsymbol{\eta}_a(\mathbf{x}_k)) \cdot \frac{\partial \mathbf{h}^a(\mathbf{x}_k)}{\partial \theta_i},
\end{aligned}$$

where we note that $F'_a(\mathbf{h}(\mathbf{x}_k)) = \boldsymbol{\eta}_a(\mathbf{x}_k)$ which follows from the connection to expected parameters and partition functions of exponential families, see *e.g.* (Soen & Sun, 2021).

Then Eq. (5) follows immediately. \square

G.II Eq. (6)

Proof. For Eq. (6), we also calculate the derivative:

$$\begin{aligned}
\frac{\partial \log p(\mathbf{y}_k | \mathbf{x}_k)}{\partial \theta_i} &= \frac{\partial}{\partial \theta_i} (\mathbf{t}^\top(\mathbf{y}_k) \mathbf{h}(\mathbf{x}_k) - F(\mathbf{h}(\mathbf{x}_k))) \\
&= \mathbf{t}_a(\mathbf{y}_k) \cdot \frac{\partial \mathbf{h}^a(\mathbf{x}_k)}{\partial \theta_i} - \frac{\partial F(\mathbf{h}(\mathbf{x}_k))}{\partial \theta_i}.
\end{aligned}$$

Then

$$\begin{aligned}
\frac{\partial^2 \log p(\mathbf{y}_k | \mathbf{x}_k)}{\partial^2 \theta_i} &= \frac{\partial}{\partial \theta_i} \left(\mathbf{t}_a(\mathbf{y}_k) \cdot \frac{\partial \mathbf{h}^a(\mathbf{x}_k)}{\partial \theta_i} - \frac{\partial F(\mathbf{h}(\mathbf{x}_k))}{\partial \theta_i} \right) \\
&= \mathbf{t}_a(\mathbf{y}_k) \cdot \frac{\partial^2 \mathbf{h}^a(\mathbf{x}_k)}{\partial^2 \theta_i} - \frac{\partial^2 F(\mathbf{h}(\mathbf{x}_k))}{\partial^2 \theta_i}.
\end{aligned}$$

Then Eq. (6) follows immediately. \square

Remark G.1. Although Eq. (6) is useful in practice, *i.e.*, it states an equation which can be calculated via automatic differentiation, in the appendix and proofs we use an alternative equation. In particular, we use

$$\begin{aligned}
\hat{\mathcal{I}}_2(\theta_i) &= \frac{1}{N} \sum_{k=1}^N \left((\boldsymbol{\eta}_a(\mathbf{x}_k) - \mathbf{t}_a(\mathbf{y}_k)) \cdot \frac{\partial^2 \mathbf{h}^a(\mathbf{x}_k)}{\partial^2 \theta_i} \right. \\
&\quad \left. + \frac{\partial \mathbf{h}^a(\mathbf{x}_k)}{\partial \theta_i} \cdot \mathcal{I}_{ab}(\mathbf{h} | \mathbf{x}_k) \cdot \frac{\partial \mathbf{h}^b(\mathbf{x}_k)}{\partial \theta_i} \right),
\end{aligned}$$

which follows from taking the derivative of $\partial_i \log p(\mathbf{y}_k | \mathbf{x}_k)$ in the proof of Eq. (5) (above).

H Proof of Eq. (10)

We first begin by proving the follow lemma to bound an $\mathfrak{R}^{n \times n}$ matrix.

Lemma H.1. Let $A \in \mathfrak{R}^{n \times n}$ and $\mathbf{v} \in \mathfrak{R}^n$, then

$$\|\mathbf{v}\|_2^2 \cdot \lambda_{\min}(A) \leq \mathbf{v}^a \mathbf{v}^b A_{ab} \leq \|\mathbf{v}\|_2^2 \cdot \lambda_{\max}(A).$$

Proof. The proof follows immediately from the Courant-Fischer min-max theorem (Tao, 2012). That is,

$$\begin{aligned} \lambda_{\min}(A) &= \inf_{\mathbf{u}: \|\mathbf{u}\|=1} \mathbf{u}^a \mathbf{u}^b A_{ab}; \\ \lambda_{\max}(A) &= \sup_{\mathbf{u}: \|\mathbf{u}\|=1} \mathbf{u}^a \mathbf{u}^b A_{ab}. \end{aligned}$$

Thus it follows that:

$$\begin{aligned} \mathbf{v}^a \mathbf{v}^b A_{ab} &= \|\mathbf{v}\|_2^2 \cdot (\mathbf{v}/\|\mathbf{v}\|_2)^a (\mathbf{v}/\|\mathbf{v}\|_2)^b A_{ab} \\ &\leq \|\mathbf{v}\|_2^2 \lambda_{\max}(A). \end{aligned}$$

The lower bound follows identically.

We note that this can be similarly proven via trace bounds, *e.g.*, (Wang et al., 1986). \square

Now we can prove Eq. (10).

Proof. The proof follows from Lemma A.1, Eq. (23), and directly applying Lemma H.1. \square

I Proof of Eq. (11)

Let us first define the maximum and minimum Z-eigenvalues of a 4-dimensional tensor \mathcal{K} .

$$\tilde{\lambda}_{\min}(\mathcal{K}) = \inf_{\mathbf{u}: \|\mathbf{u}\|_2=1} \mathbf{u}^a \mathbf{u}^b \mathbf{u}^c \mathbf{u}^d \mathcal{K}_{abcd}; \quad (33)$$

$$\tilde{\lambda}_{\max}(\mathcal{K}) = \sup_{\mathbf{u}: \|\mathbf{u}\|_2=1} \mathbf{u}^a \mathbf{u}^b \mathbf{u}^c \mathbf{u}^d \mathcal{K}_{abcd}. \quad (34)$$

Now We first prove the following lemma regarding the Z-eigenvalues.

Lemma I.1. Suppose \mathcal{K} is 4-dimensional tensor. Then we have

$$\|\mathbf{v}\|_2^4 \cdot \tilde{\lambda}_{\min}(\mathcal{K}) \leq \mathbf{v}^a \mathbf{v}^b \mathbf{v}^c \mathbf{v}^d \mathcal{K}_{abcd} \leq \|\mathbf{v}\|_2^4 \cdot \tilde{\lambda}_{\max}(\mathcal{K}) \quad (35)$$

Proof. The proof follows similarly to Lemma H.1. We simple use the following calculation:

$$\begin{aligned} &\mathbf{v}^a \mathbf{v}^b \mathbf{v}^c \mathbf{v}^d \mathcal{K}_{abcd} \\ &= \|\mathbf{v}\|_2^4 \cdot (\mathbf{v}/\|\mathbf{v}\|_2)^a (\mathbf{v}/\|\mathbf{v}\|_2)^b (\mathbf{v}/\|\mathbf{v}\|_2)^c (\mathbf{v}/\|\mathbf{v}\|_2)^d \mathcal{K}_{abcd} \\ &\leq \|\mathbf{v}\|_2^4 \cdot \sup_{\mathbf{u}: \|\mathbf{u}\|_2=1} \mathbf{u}^a \mathbf{u}^b \mathbf{u}^c \mathbf{u}^d \mathcal{K}_{abcd} \\ &= \|\mathbf{v}\|_2^4 \cdot \tilde{\lambda}_{\max}(\mathcal{K}). \end{aligned}$$

The minimum case is proven identically (with the opposite inequality). \square

Now we can prove the bounds of Eq. (11)

Proof. From Lemma A.1, we have that

$$\mathcal{V}_1(\theta_i | \mathbf{x}) = \frac{1}{N} \partial_i \mathbf{h}^a(\mathbf{x}) \partial_i \mathbf{h}^b(\mathbf{x}) \partial_i \mathbf{h}^c(\mathbf{x}) \partial_i \mathbf{h}^d(\mathbf{x}) [\mathcal{K}_{abcd} - \mathcal{I}_{ab}(\mathbf{h} | \mathbf{x}) \cdot \mathcal{I}_{cd}(\mathbf{h} | \mathbf{x})],$$

where we shorthand $\mathcal{K}_{abcd} = \mathcal{K}_{abcd}^p(\mathbf{t} | \mathbf{x})$

We bound two terms.

$$\begin{aligned} \|\partial_i \mathbf{h}(\mathbf{x})\|_2^4 \cdot \tilde{\lambda}_{\min}(\mathcal{K}) &\leq \partial_i \mathbf{h}^a(\mathbf{x}) \partial_i \mathbf{h}^b(\mathbf{x}) \partial_i \mathbf{h}^c(\mathbf{x}) \partial_i \mathbf{h}^d(\mathbf{x}) \mathcal{K}_{abcd} \\ &\leq \|\partial_i \mathbf{h}(\mathbf{x})\|_2^4 \cdot \tilde{\lambda}_{\max}(\mathcal{K}), \end{aligned}$$

which follows directly from Lemma I.1

We now bound the second term in a similar way, taking $v^a := \partial_i \mathbf{h}^a(\mathbf{x})$ and noting that

$$v^a v^b v^c v^d \mathcal{I}_{ab}(\mathbf{h} | \mathbf{x}) \mathcal{I}_{cd}(\mathbf{h} | \mathbf{x}) = (v^a v^b \mathcal{I}_{ab}(\mathbf{h} | \mathbf{x}))^2$$

which directly gives us,

$$\begin{aligned} (\|v\|_2^2 \cdot \lambda_{\min}(\mathcal{I}(\mathbf{h} | \mathbf{x})))^2 &\leq v^a v^b v^c v^d \mathcal{I}_{ab}(\mathbf{h} | \mathbf{x}) \mathcal{I}_{cd}(\mathbf{h} | \mathbf{x}) \\ &\leq (\|v\|_2^2 \cdot \lambda_{\max}(\mathcal{I}(\mathbf{h} | \mathbf{x})))^2. \end{aligned}$$

which follows from Lemma H.1.

Thus, together these bounds prove Eq. (11). □

J Proof of Eq. (12)

From Lemma A.1 we have that,

$$\mathcal{V}_2^i = \frac{1}{N} \partial_{ii}^2 \mathbf{h}^a(\mathbf{x}) \partial_{ii}^2 \mathbf{h}^b(\mathbf{x}) \mathcal{I}_{ab}(\mathbf{h}_L).$$

Thus, short-handing $h^a := \partial_{ii}^2 \mathbf{h}^a(\mathbf{x})$, we get

$$\|h\|_2^2 \cdot \lambda_{\min}(\mathcal{I}(\mathbf{h})) \leq h^a h^b \cdot \mathcal{I}_{ab}(\mathbf{h}) \leq \|h\|_2^2 \cdot \lambda_{\max}(\mathcal{I}(\mathbf{h})),$$

which follows from Lemma H.1. This immediately gives the bound as required.

K Proof of Corollary 4.2

Proof. The corollary holds from distributing the inf or sup and examining how the variational definition of the generalized ‘eigenvalue’ simplifies under tensor products.

Indeed, for the minimum case,

$$\begin{aligned}
& \tilde{\lambda}_{\min} (\mathcal{K}^p(\mathbf{t} | \mathbf{x}) - \mathcal{I}(\mathbf{h} | \mathbf{x}) \otimes \mathcal{I}(\mathbf{h} | \mathbf{x})) \\
&= \inf_{\mathbf{u}: \|\mathbf{u}\|_2=1} \mathbf{u}^a \mathbf{u}^b \mathbf{u}^c \mathbf{u}^d (\mathcal{K}_{abcd}^p(\mathbf{t} | \mathbf{x}) - \mathcal{I}_{ab}(\mathbf{h} | \mathbf{x}) \cdot \mathcal{I}_{cd}(\mathbf{h} | \mathbf{x})) \\
&\geq \left(\inf_{\mathbf{u}: \|\mathbf{u}\|_2=1} \mathbf{u}^a \mathbf{u}^b \mathbf{u}^c \mathbf{u}^d \mathcal{K}_{abcd}^p(\mathbf{t} | \mathbf{x}) \right) + \left(\inf_{\mathbf{u}: \|\mathbf{u}\|_2=1} \mathbf{u}^a \mathbf{u}^b \mathbf{u}^c \mathbf{u}^d (-\mathcal{I}_{ab}(\mathbf{h} | \mathbf{x}) \cdot \mathcal{I}_{cd}(\mathbf{h} | \mathbf{x})) \right) \\
&= \left(\inf_{\mathbf{u}: \|\mathbf{u}\|_2=1} \mathbf{u}^a \mathbf{u}^b \mathbf{u}^c \mathbf{u}^d \mathcal{K}_{abcd}^p(\mathbf{t} | \mathbf{x}) \right) - \left(\sup_{\mathbf{u}: \|\mathbf{u}\|_2=1} \mathbf{u}^a \mathbf{u}^b \mathbf{u}^c \mathbf{u}^d (\mathcal{I}_{ab}(\mathbf{h} | \mathbf{x}) \cdot \mathcal{I}_{cd}(\mathbf{h} | \mathbf{x})) \right) \\
&= \left(\inf_{\mathbf{u}: \|\mathbf{u}\|_2=1} \mathbf{u}^a \mathbf{u}^b \mathbf{u}^c \mathbf{u}^d \mathcal{K}_{abcd}^p(\mathbf{t} | \mathbf{x}) \right) - \left(\sup_{\mathbf{u}: \|\mathbf{u}\|_2=1} (\mathbf{u}^a \mathbf{u}^b \mathcal{I}_{ab}(\mathbf{h} | \mathbf{x}))^2 \right) \\
&\geq \left(\inf_{\mathbf{u}: \|\mathbf{u}\|_2=1} \mathbf{u}^a \mathbf{u}^b \mathbf{u}^c \mathbf{u}^d \mathcal{K}_{abcd}^p(\mathbf{t} | \mathbf{x}) \right) - \left(\sup_{\mathbf{u}: \|\mathbf{u}\|_2=1} \mathbf{u}^a \mathbf{u}^b \mathcal{I}_{ab}(\mathbf{h} | \mathbf{x}) \right)^2,
\end{aligned}$$

where the last line holds from the fact that $\mathcal{I}_{ab}(\mathbf{h} | \mathbf{x})$ is PSD (thus the inner Einstein summation is always positive).

Taking definitions of the types of eigenvalues, gives the statement.

We note that the ‘max’ case follows identically.

Additionally, for the lower bound, we can show the non-triviality of the non-negativity of the minimum eigenvalue.

We note that $\mathcal{K}_{abcd}^p(\mathbf{t} | \mathbf{x}) = \mathbb{E}_p[\mathbf{v}_a \mathbf{v}_b \mathbf{v}_c \mathbf{v}_d]$, where $\mathbf{v} = \mathbf{t}(\mathbf{y}) - \eta(\mathbf{x})$.

Thus we have that

$$\begin{aligned}
& \tilde{\lambda}_{\min} (\mathcal{K}^p(\mathbf{t} | \mathbf{x}) - \mathcal{I}(\mathbf{h} | \mathbf{x}) \otimes \mathcal{I}(\mathbf{h} | \mathbf{x})) \\
&= \inf_{\mathbf{u}: \|\mathbf{u}\|_2=1} \mathbf{u}^a \mathbf{u}^b \mathbf{u}^c \mathbf{u}^d (\mathcal{K}_{abcd}^p(\mathbf{t} | \mathbf{x}) - \mathcal{I}_{ab}(\mathbf{h} | \mathbf{x}) \cdot \mathcal{I}_{cd}(\mathbf{h} | \mathbf{x})) \\
&= \inf_{\mathbf{u}: \|\mathbf{u}\|_2=1} \mathbb{E}_p \left[\mathbf{u}^a \mathbf{u}^b \mathbf{u}^c \mathbf{u}^d (\mathbf{v}_a \mathbf{v}_b \mathbf{v}_c \mathbf{v}_d - \mathcal{I}_{ab}(\mathbf{h} | \mathbf{x}) \cdot \mathcal{I}_{cd}(\mathbf{h} | \mathbf{x})) \right] \\
&= \inf_{\mathbf{u}: \|\mathbf{u}\|_2=1} \mathbb{E}_p \left[(\mathbf{u}^a \mathbf{u}^b (\mathbf{v}_a \mathbf{v}_b - \mathcal{I}_{ab}(\mathbf{h} | \mathbf{x})))^2 \right] \geq 0.
\end{aligned}$$

Equality holds from simply looking at the definition of $\mathcal{K}^p(\mathbf{t} | \mathbf{x})$ and $\mathcal{I}(\mathbf{h} | \mathbf{x})$ (as moments). \square

L Proof of Proposition 4.3

Proof. Letting $\mathbf{v} = \mathbf{t}(y) - \boldsymbol{\eta}(y)$, we note that the maximum eigenvalue is given by,

$$\begin{aligned}
\lambda_{\max}(\mathcal{K}^p(\mathbf{t} | \mathbf{x})) &= \sup_{\mathbf{u}: \|\mathbf{u}\|_2=1} \mathbf{u}^a \mathbf{u}^b \mathbf{u}^c \mathbf{u}^d \mathcal{K}_{abcd}^p(\mathbf{t} | \mathbf{x}) \\
&= \sup_{\mathbf{u}: \|\mathbf{u}\|_2=1} \mathbb{E}^p [\mathbf{u}^a \mathbf{u}^b \mathbf{u}^c \mathbf{u}^d \mathbf{v}_a \mathbf{v}_b \mathbf{v}_c \mathbf{v}_d] \\
&= \sup_{\mathbf{u}: \|\mathbf{u}\|_2=1} \mathbb{E}^p [(\mathbf{u}^\top \mathbf{v})^4] \\
&= \sup_{\mathbf{u}: \|\mathbf{u}\|_2=1} \mathbb{E}^p [(\mathbf{u}^\top \mathbf{v})^2 (\mathbf{u}^\top \mathbf{v})^2] \\
&\leq \sup_{\mathbf{u}: \|\mathbf{u}\|_2=1} \mathbb{E}^p [(\|\mathbf{u}\|_2 \cdot \|\mathbf{v}\|_2)^2 (\mathbf{u}^\top \mathbf{v})^2] \\
&\leq B \cdot \sup_{\mathbf{u}: \|\mathbf{u}\|_2=1} \mathbb{E}^p [(\mathbf{u}^\top \mathbf{v})^2] \\
&= B \cdot \lambda_{\max}(\mathcal{I}(\mathbf{h} | \mathbf{x})).
\end{aligned}$$

□

M Proof of Corollary 4.6

Proof. We split up the proof into the two arguments of the various min-function.

For the right term:

Suppose that we have a bound such that $\mathcal{V}_j(\theta_i | \mathbf{x}) \leq \alpha \beta_i$. Then,

$$\begin{aligned}
\|\mathcal{V}_j(\boldsymbol{\theta} | \mathbf{x})\|_2^2 &= \sum_{i=1}^{\dim(\boldsymbol{\theta})} (\mathcal{V}_j(\theta_i | \mathbf{x}))^2 \\
&\leq \sum_{i=1}^{\dim(\boldsymbol{\theta})} (\alpha \beta_i)^2 \\
&= \alpha^2 \sum_{i=1}^{\dim(\boldsymbol{\theta})} \beta_i^2.
\end{aligned}$$

Thus we have,

$$\|\mathcal{V}_j(\boldsymbol{\theta} | \mathbf{x})\|_2 \leq \alpha \sqrt{\sum_{i=1}^{\dim(\boldsymbol{\theta})} \beta_i^2}.$$

Taking the appropriate α and β from Eqs. (11) and (12) proves the case for Eqs. (17) and (19). For Eq. (18), that is taking

$$\begin{aligned}
\alpha &= \frac{1}{N} \cdot \left(\tilde{\lambda}_{\max}(\mathcal{K}^p(\mathbf{t} | \mathbf{x})) - \lambda_{\min}^2(\mathcal{I}(\mathbf{h} | \mathbf{x})) \right); \\
\beta_i &= \|\partial_i \mathbf{h}(\mathbf{x})\|_2^4.
\end{aligned}$$

Where we note that

$$\begin{aligned}
\sqrt{\sum_{i=1}^{\dim(\boldsymbol{\theta})} (\|\partial_i \mathbf{h}(\mathbf{x})\|_2^4)^2} &= \sqrt{\sum_{i=1}^{\dim(\boldsymbol{\theta})} \left[\left(\sum_{t=1}^T [\partial_i h_t(\mathbf{x})]^2 \right)^2 \right]} \\
&= \sqrt{\sum_{i=1}^{\dim(\boldsymbol{\theta})} \left(\sum_{t=1}^T [\partial_i h_t(\mathbf{x})]^2 \right)^4} \\
&\leq \sqrt{\left(\sum_{i=1}^{\dim(\boldsymbol{\theta})} \sum_{t=1}^T [\partial_i h_t(\mathbf{x})]^2 \right)^4} \\
&= \left(\sum_{i=1}^{\dim(\boldsymbol{\theta})} \sum_{t=1}^T [\partial_i h_t(\mathbf{x})]^2 \right)^2 \\
&= \|\partial \mathbf{h}(\mathbf{x})\|_F^4.
\end{aligned}$$

For Eq. (19), that is taking

$$\begin{aligned}
\alpha &= \frac{1}{N} \cdot \lambda_{\max}(\mathcal{I}(\mathbf{h} | \mathbf{x})); \\
\beta_i &= \|\partial_{ii}^2 \mathbf{h}(\mathbf{x})\|_2^2.
\end{aligned}$$

Where we note that

$$\begin{aligned}
\sqrt{\sum_{i=1}^{\dim(\boldsymbol{\theta})} (\|\partial_{ii}^2 \mathbf{h}(\mathbf{x})\|_2^2)^2} &= \sqrt{\sum_{i=1}^{\dim(\boldsymbol{\theta})} \left(\sum_{t=1}^T [\partial_{ii}^2 h_t(\mathbf{x})]^2 \right)^2} \\
&\leq \sqrt{\left(\sum_{i=1}^{\dim(\boldsymbol{\theta})} \sum_{t=1}^T [\partial_{ii}^2 h_t(\mathbf{x})]^2 \right)^2} \\
&= \sum_{i=1}^{\dim(\boldsymbol{\theta})} \sum_{t=1}^T [\partial_{ii}^2 h_t(\mathbf{x})]^2 \\
&= \|\text{dHes}(\mathbf{h} | \mathbf{x})\|_F^2.
\end{aligned}$$

For the left term:

We take the largest singular value of the network derivative term. We then further notice that $s_{\max}(A) \leq \|A\|_F$ from norm ordering (of the matrix 2-norm).

To further elaborate on the Eq. (18) case, we further need to simplify the following:

$$\begin{aligned}
s_{\max}(\text{vJac}) &\leq \|\text{vJac}(\mathbf{h} | \mathbf{x})\|_F \\
&= \sqrt{\sum_{i=1}^{\dim(\boldsymbol{\theta})} \|\partial_i \mathbf{h}(\mathbf{x}) \partial_i \mathbf{h}^\top(\mathbf{x})\|_F^2} \\
&= \sqrt{\sum_{a,b=1}^T \sum_{i=1}^{\dim(\boldsymbol{\theta})} (\partial_i \mathbf{h}^a(\mathbf{x}))^2 (\partial_i \mathbf{h}^b(\mathbf{x}))^2} \\
&\leq \sqrt{\sum_{a,b=1}^T \|(\partial \mathbf{h}^a(\mathbf{x}))^2\|_2 \cdot \|(\partial \mathbf{h}^b(\mathbf{x}))^2\|_2} \\
&= \sqrt{\left(\sum_{a=1}^T \|(\partial \mathbf{h}^a(\mathbf{x}))^2\|_2 \right)^2} \\
&= \sum_{a=1}^T \|(\partial \mathbf{h}^a(\mathbf{x}))^2\|_2 \\
&= \sum_{a=1}^T \sqrt{\sum_{i=1}^{\dim(\boldsymbol{\theta})} (\partial_i \mathbf{h}^a(\mathbf{x}))^4} \\
&\leq \sum_{a=1}^T \sum_{i=1}^{\dim(\boldsymbol{\theta})} |(\partial_i \mathbf{h}^a(\mathbf{x}))^2| \\
&= \|\partial \mathbf{h}(\mathbf{x})\|_F^2,
\end{aligned}$$

where the last inequality follows from the norm ordering $\|\cdot\|_2 \leq \|\cdot\|_1$. \square

N Proof of Theorem 4.7

The proof follows from the law of total variances directly. However, we also show how to directly prove the theorem for each estimator individually.

For $\mathcal{V}_1(\boldsymbol{\theta})$

Proof.

$$\mathcal{V}_1(\theta_i) = \frac{1}{N} \left(\mathbb{E}_{p(\mathbf{x}, \mathbf{y})} \left[\left(\frac{\partial \log p(\mathbf{y} | \mathbf{x})}{\partial \theta_i} \right)^2 \right] - \mathbb{E}_{p(\mathbf{x}, \mathbf{y})} \left[\frac{\partial \log p(\mathbf{y} | \mathbf{x})}{\partial \theta_i} \right]^2 \right).$$

Let $\delta_a(\mathbf{x}, \mathbf{y}) := (\mathbf{t}(\mathbf{y}) - \boldsymbol{\eta}(\mathbf{x}))$.

$$\begin{aligned}
& \mathbb{E}_{p(\mathbf{x}, \mathbf{y})} \left[\left(\frac{\partial \log p(\mathbf{y} | \mathbf{x})}{\partial \theta_i} \right)^2 \right] \\
&= \mathbb{E}_{p(\mathbf{x}, \mathbf{y})} \left[\frac{\partial \mathbf{h}^a(\mathbf{x})}{\partial \theta_i} \frac{\partial \mathbf{h}^b(\mathbf{x})}{\partial \theta_i} \frac{\partial \mathbf{h}^c(\mathbf{x})}{\partial \theta_i} \frac{\partial \mathbf{h}^d(\mathbf{x})}{\partial \theta_i} \delta_a(\mathbf{x}, \mathbf{y}) \delta_b(\mathbf{x}, \mathbf{y}) \delta_c(\mathbf{x}, \mathbf{y}) \delta_d(\mathbf{x}, \mathbf{y}) \right] \\
&= \mathbb{E}_{q(\mathbf{x})} \left[\frac{\partial \mathbf{h}^a(\mathbf{x})}{\partial \theta_i} \frac{\partial \mathbf{h}^b(\mathbf{x})}{\partial \theta_i} \frac{\partial \mathbf{h}^c(\mathbf{x})}{\partial \theta_i} \frac{\partial \mathbf{h}^d(\mathbf{x})}{\partial \theta_i} \mathbb{E}_{p(\mathbf{y} | \mathbf{x})} [\delta_a(\mathbf{x}, \mathbf{y}) \delta_b(\mathbf{x}, \mathbf{y}) \delta_c(\mathbf{x}, \mathbf{y}) \delta_d(\mathbf{x}, \mathbf{y})] \right] \\
&= \mathbb{E}_{q(\mathbf{x})} \left[\frac{\partial \mathbf{h}^a(\mathbf{x})}{\partial \theta_i} \frac{\partial \mathbf{h}^b(\mathbf{x})}{\partial \theta_i} \frac{\partial \mathbf{h}^c(\mathbf{x})}{\partial \theta_i} \frac{\partial \mathbf{h}^d(\mathbf{x})}{\partial \theta_i} \mathcal{K}_{abcd}^p(\mathbf{t} | \mathbf{x}) \right]
\end{aligned}$$

And:

$$\begin{aligned}
& \mathbb{E}_{p(\mathbf{x}, \mathbf{y})} \left[\frac{\partial \log p(\mathbf{y} | \mathbf{x})}{\partial \theta_i} \right]^2 \\
&= \mathbb{E}_{p(\mathbf{x}, \mathbf{y})} \left[\frac{\partial \mathbf{h}^a(\mathbf{x})}{\partial \theta_i} \frac{\partial \mathbf{h}^b(\mathbf{x})}{\partial \theta_i} \delta_a(\mathbf{x}, \mathbf{y}) \delta_b(\mathbf{x}, \mathbf{y}) \right]^2 \\
&= \mathbb{E}_{q(\mathbf{x})} \left[\frac{\partial \mathbf{h}^a(\mathbf{x})}{\partial \theta_i} \frac{\partial \mathbf{h}^b(\mathbf{x})}{\partial \theta_i} \mathbb{E}_{p(\mathbf{y} | \mathbf{x})} [\delta_a(\mathbf{x}, \mathbf{y}) \delta_b(\mathbf{x}, \mathbf{y})] \right]^2 \\
&= \mathbb{E}_{q(\mathbf{x})} \left[\frac{\partial \mathbf{h}^a(\mathbf{x})}{\partial \theta_i} \frac{\partial \mathbf{h}^b(\mathbf{x})}{\partial \theta_i} \mathcal{I}_{ab}(\mathbf{h} | \mathbf{x}) \right]^2 \\
&= \mathbb{E}_{q(\mathbf{x})} \left[\left(\frac{\partial \mathbf{h}^a(\mathbf{x})}{\partial \theta_i} \frac{\partial \mathbf{h}^b(\mathbf{x})}{\partial \theta_i} \mathcal{I}_{ab}(\mathbf{h} | \mathbf{x}) \right)^2 \right] - \text{Var}_{\mathbf{X}} \left(\left(\frac{\partial \mathbf{h}(\mathbf{x})}{\partial \theta_i} \right)^\top \mathcal{I}(\mathbf{h} | \mathbf{x}) \frac{\partial \mathbf{h}(\mathbf{x})}{\partial \theta_i} \right) \\
&= \mathbb{E}_{q(\mathbf{x})} \left[\left(\frac{\partial \mathbf{h}^a(\mathbf{x})}{\partial \theta_i} \frac{\partial \mathbf{h}^b(\mathbf{x})}{\partial \theta_i} \mathcal{I}_{ab}(\mathbf{h} | \mathbf{x}) \right)^2 \right] - \text{Var}_{\mathbf{X}}(\mathcal{I}(\theta_i | \mathbf{x})).
\end{aligned}$$

Together:

$$\begin{aligned}
\mathcal{V}_1(\theta_i) &= \frac{1}{N} \text{Var}_{\mathbf{X}}(\mathcal{I}(\theta_i | \mathbf{x})) \\
&+ \frac{1}{N} \mathbb{E}_{q(\mathbf{x})} \left[\frac{\partial \mathbf{h}^a(\mathbf{x})}{\partial \theta_i} \frac{\partial \mathbf{h}^b(\mathbf{x})}{\partial \theta_i} \frac{\partial \mathbf{h}^c(\mathbf{x})}{\partial \theta_i} \frac{\partial \mathbf{h}^d(\mathbf{x})}{\partial \theta_i} [\mathcal{K}_{abcd}^p(\mathbf{t} | \mathbf{x}) - \mathcal{I}_{ab}(\mathbf{h} | \mathbf{x}) \cdot \mathcal{I}_{cd}(\mathbf{h} | \mathbf{x})] \right]
\end{aligned}$$

□

For $\mathcal{V}_2(\boldsymbol{\theta})$

Proof.

$$\begin{aligned}
\mathcal{V}_2(\theta_i) &= \frac{1}{N} \text{Var} \left((\boldsymbol{\eta}_a(\mathbf{x}) - \mathbf{t}_a(\mathbf{y})) \frac{\partial^2 \mathbf{h}^a(\mathbf{x})}{\partial \theta_i \partial \theta_i} + \mathcal{I}(\theta_i | \mathbf{x}) \right) \\
&= \frac{1}{N} \left[\underbrace{\text{Var} \left((\boldsymbol{\eta}_a(\mathbf{x}) - \mathbf{t}_a(\mathbf{y})) \frac{\partial^2 \mathbf{h}^a(\mathbf{x})}{\partial \theta_i \partial \theta_i} \right)}_{(a)} + \text{Var}(\mathcal{I}(\theta_i | \mathbf{x})) \right. \\
&\quad \left. + 2 \underbrace{\text{Cov} \left((\boldsymbol{\eta}_a(\mathbf{x}) - \mathbf{t}_a(\mathbf{y})) \frac{\partial^2 \mathbf{h}^a(\mathbf{x})}{\partial \theta_i \partial \theta_i}, \mathcal{I}(\theta_i | \mathbf{x}) \right)}_{(b)} \right].
\end{aligned}$$

$$\begin{aligned}
(a) &= \text{Var} \left((\boldsymbol{\eta}_a(\mathbf{x}) - \mathbf{t}_a(\mathbf{y})) \frac{\partial^2 \mathbf{h}^a(\mathbf{x})}{\partial \theta_i \partial \theta_i} \right) \\
&= \mathbb{E}_{p(\mathbf{x}, \mathbf{y})} \left[\left((\boldsymbol{\eta}_a(\mathbf{x}) - \mathbf{t}_a(\mathbf{y})) \frac{\partial^2 \mathbf{h}^a(\mathbf{x})}{\partial \theta_i \partial \theta_i} \right)^2 \right] \\
&\quad - \mathbb{E}_{p(\mathbf{x}, \mathbf{y})} \left[(\boldsymbol{\eta}_a(\mathbf{x}) - \mathbf{t}_a(\mathbf{y})) \frac{\partial^2 \mathbf{h}^a(\mathbf{x})}{\partial \theta_i \partial \theta_i} \right]^2 \\
&= \mathbb{E}_{p(\mathbf{x}, \mathbf{y})} \left[\left((\boldsymbol{\eta}_a(\mathbf{x}) - \mathbf{t}_a(\mathbf{y})) \frac{\partial^2 \mathbf{h}^a(\mathbf{x})}{\partial \theta_i \partial \theta_i} \right)^2 \right] \\
&\quad - \mathbb{E}_{q(\mathbf{x})} \left[\frac{\partial^2 \mathbf{h}^a(\mathbf{x})}{\partial \theta_i \partial \theta_i} \mathbb{E}_{p(\mathbf{y} | \mathbf{x})} [(\boldsymbol{\eta}_a(\mathbf{x}) - \mathbf{t}_a(\mathbf{y}))] \right]^2 \\
&= \mathbb{E}_{p(\mathbf{x}, \mathbf{y})} \left[\left((\boldsymbol{\eta}_a(\mathbf{x}) - \mathbf{t}_a(\mathbf{y})) \frac{\partial^2 \mathbf{h}^a(\mathbf{x})}{\partial \theta_i \partial \theta_i} \right)^2 \right] - 0 \\
&= \mathbb{E}_{q(\mathbf{x})} \left[\left(\frac{\partial^2 \mathbf{h}(\mathbf{x})}{\partial \theta_i \partial \theta_i} \right)^\top \mathbb{E}_{p(\mathbf{y} | \mathbf{x})} [(\boldsymbol{\eta}(\mathbf{x}) - \mathbf{t}(\mathbf{y})) (\boldsymbol{\eta}(\mathbf{x}) - \mathbf{t}(\mathbf{y}))^\top] \left(\frac{\partial^2 \mathbf{h}(\mathbf{x})}{\partial \theta_i \partial \theta_i} \right) \right] \\
&= \mathbb{E}_{q(\mathbf{x})} \left[\left(\frac{\partial^2 \mathbf{h}(\mathbf{x})}{\partial \theta_i \partial \theta_i} \right)^\top \mathcal{I}(\mathbf{h} | \mathbf{x}) \left(\frac{\partial^2 \mathbf{h}(\mathbf{x})}{\partial \theta_i \partial \theta_i} \right) \right].
\end{aligned}$$

$$\begin{aligned}
(b) &= \text{Cov} \left((\boldsymbol{\eta}_a(\mathbf{x}) - \mathbf{t}_a(\mathbf{y})) \frac{\partial^2 \mathbf{h}^a(\mathbf{x})}{\partial \theta_i \partial \theta_i}, \mathcal{I}(\theta_i | \mathbf{x}) \right) \\
&= \mathbb{E}_{p(\mathbf{x}, \mathbf{y})} \left[(\boldsymbol{\eta}_a(\mathbf{x}) - \mathbf{t}_a(\mathbf{y})) \frac{\partial^2 \mathbf{h}^a(\mathbf{x})}{\partial \theta_i \partial \theta_i} \mathcal{I}(\theta_i | \mathbf{x}) \right] \\
&\quad - \mathbb{E}_{p(\mathbf{x}, \mathbf{y})} \left[(\boldsymbol{\eta}_a(\mathbf{x}) - \mathbf{t}_a(\mathbf{y})) \frac{\partial^2 \mathbf{h}^a(\mathbf{x})}{\partial \theta_i \partial \theta_i} \right] \mathbb{E}_{p(\mathbf{x}, \mathbf{y})} [\mathcal{I}(\theta_i | \mathbf{x})] \\
&= 0,
\end{aligned}$$

which follows by taking the ‘partial’ expectation ($\mathbf{y} | \mathbf{x}$) for both terms.

Thus together,

$$\mathcal{V}_2(\theta_i) = \frac{1}{N} \text{Var}(\mathcal{I}(\theta_i | \mathbf{x})) + \frac{1}{N} \mathbb{E}_{q(\mathbf{x})} \left[\left(\frac{\partial^2 \mathbf{h}(\mathbf{x})}{\partial \theta_i \partial \theta_i} \right)^\top \mathcal{I}(\mathbf{h} | \mathbf{x}) \left(\frac{\partial^2 \mathbf{h}(\mathbf{x})}{\partial \theta_i \partial \theta_i} \right) \right].$$

□

O Proof of Lemma 4.8

Proof. The lower bound holds from just considering the non-negativity of variance. For the upper bound, we utilize the bound directly consider the bounds of Eq. (10),

$$\begin{aligned} \text{Var}(\mathcal{I}(\theta_i | \mathbf{x})) &= \mathbb{E}_{q(\mathbf{x})} [\mathcal{I}(\theta_i | \mathbf{x})^2] - \mathbb{E}_{q(\mathbf{x})} [\mathcal{I}(\theta_i | \mathbf{x})]^2 \\ &= \mathbb{E}_{q(\mathbf{x})} [\mathcal{I}(\theta_i | \mathbf{x})^2] \\ &= \mathbb{E}_{q(\mathbf{x})} [\|\partial_i \mathbf{h}(\mathbf{x})\|_2^4 \cdot \lambda_{\max}^2(\mathcal{I}(\mathbf{h} | \mathbf{x}))]. \end{aligned}$$

□

P Proof of Proposition 5.1

We first derive the statistics $\mathcal{I}(\mathbf{h} | \mathbf{x})$ and $\mathcal{K}^p(\mathbf{t} | \mathbf{x})$ presented in Section 5.1. It follows that from the regression setting, we have that,

$$\begin{aligned} F(\mathbf{h}(\mathbf{x})) &= \log \int \pi(\mathbf{y}) \cdot \exp(\mathbf{t}^\top(\mathbf{y})\mathbf{h}(\mathbf{x})) \\ &= \log \int \pi(\mathbf{y}) \cdot \exp(\mathbf{y}^\top \mathbf{h}(\mathbf{x})), \end{aligned}$$

where notably, by definition, $\pi(\mathbf{y})$ is independent of learned parameter $\mathbf{h}(\mathbf{x})$.

As such, we have that:

$$\frac{\partial}{\partial \mathbf{h}_i} F(\mathbf{h}) \Big|_{\mathbf{h}=\mathbf{h}(\mathbf{x})} = \frac{1}{\int \pi(\mathbf{y}) \cdot \exp(\mathbf{t}^\top(\mathbf{y})\mathbf{h}(\mathbf{x}))} \cdot \int \pi(\mathbf{y}) \cdot \exp(\mathbf{t}^\top(\mathbf{y})\mathbf{h}(\mathbf{x})) \cdot \mathbf{h}_i(\mathbf{x}) = \mathbb{E}_{p(\mathbf{y} | \mathbf{x})} [\mathbf{y}_i].$$

Now we note that $\mathbb{E}_p(\mathbf{y} | \mathbf{x})[\mathbf{y}_i]$ is exactly $\mathbf{h}_i(\mathbf{x})$ as the parameter $\mathbf{h}(\mathbf{x})$ specifies the mean of the (isotropic) multivariate normal distribution. As such we have that,

$$\begin{aligned} \frac{\partial}{\partial \mathbf{h}_i} F(\mathbf{h}) \Big|_{\mathbf{h}=\mathbf{h}(\mathbf{x})} &= \mathbf{h}(\mathbf{x}) \\ \mathcal{I}(\mathbf{h} | \mathbf{x}) &= \frac{\partial^2}{\partial \mathbf{h} \partial \mathbf{h}^\top} F(\mathbf{h}) \Big|_{\mathbf{h}=\mathbf{h}(\mathbf{x})} = I. \end{aligned}$$

Furthermore, by (Soen & Sun, 2021, Lemma 5), we have that,

$$\begin{aligned} \mathcal{K}_{abcd}^p(\mathbf{t} | \mathbf{x}) &= \frac{\partial^4 F(\mathbf{h})}{\partial \mathbf{h}_a \partial \mathbf{h}_b \partial \mathbf{h}_c \partial \mathbf{h}_d} \Big|_{\mathbf{h}=\mathbf{h}(\mathbf{x})} \\ &+ \mathcal{I}_{ab}(\mathbf{h} | \mathbf{x}) \cdot \mathcal{I}_{cd}(\mathbf{h} | \mathbf{x}) + \mathcal{I}_{ac}(\mathbf{h} | \mathbf{x}) \cdot \mathcal{I}_{bd}(\mathbf{h} | \mathbf{x}) + \mathcal{I}_{ad}(\mathbf{h} | \mathbf{x}) \cdot \mathcal{I}_{bc}(\mathbf{h} | \mathbf{x}) \\ &= 0 + \mathcal{I}_{ab}(\mathbf{h} | \mathbf{x}) \cdot \mathcal{I}_{cd}(\mathbf{h} | \mathbf{x}) + \mathcal{I}_{ac}(\mathbf{h} | \mathbf{x}) \cdot \mathcal{I}_{bd}(\mathbf{h} | \mathbf{x}) + \mathcal{I}_{ad}(\mathbf{h} | \mathbf{x}) \cdot \mathcal{I}_{bc}(\mathbf{h} | \mathbf{x}) \\ &= \mathcal{I}_{ab}(\mathbf{h} | \mathbf{x}) \cdot \mathcal{I}_{cd}(\mathbf{h} | \mathbf{x}) + \mathcal{I}_{ac}(\mathbf{h} | \mathbf{x}) \cdot \mathcal{I}_{bd}(\mathbf{h} | \mathbf{x}) + \mathcal{I}_{ad}(\mathbf{h} | \mathbf{x}) \cdot \mathcal{I}_{bc}(\mathbf{h} | \mathbf{x}). \end{aligned}$$

In summary, we have,

$$\begin{aligned}\mathcal{K}_{abcd}^p(\mathbf{t} | \mathbf{x}) &= \mathcal{I}_{ab}(\mathbf{h} | \mathbf{x}) \cdot \mathcal{I}_{cd}(\mathbf{h} | \mathbf{x}) + \mathcal{I}_{ac}(\mathbf{h} | \mathbf{x}) \cdot \mathcal{I}_{bd}(\mathbf{h} | \mathbf{x}) \\ &\quad + \mathcal{I}_{ad}(\mathbf{h} | \mathbf{x}) \cdot \mathcal{I}_{bc}(\mathbf{h} | \mathbf{x}) \\ (\mathcal{K}^p(\mathbf{t} | \mathbf{x}) - \mathcal{I}(\mathbf{h} | \mathbf{x}) \otimes \mathcal{I}(\mathbf{h} | \mathbf{x}))_{abcd} &= \mathcal{I}_{ac}(\mathbf{h} | \mathbf{x}) \cdot \mathcal{I}_{bd}(\mathbf{h} | \mathbf{x}) + \mathcal{I}_{ad}(\mathbf{h} | \mathbf{x}) \cdot \mathcal{I}_{bc}(\mathbf{h} | \mathbf{x}).\end{aligned}$$

Proof. The minimum and maximum eigenvalues of $\mathcal{I}(\mathbf{h} | \mathbf{x})$ follows directly noting that the trace of a matrix is the sum of eigenvalues. As such, from the statistics presented above we have that the minimum and eigenvalue must be 1.

The tensor eigenvalues of $\mathcal{K}^p(\mathbf{t} | \mathbf{x}) - \mathcal{I}(\mathbf{h} | \mathbf{x}) \otimes \mathcal{I}(\mathbf{h} | \mathbf{x}) = \mathcal{I}_{ac}(\mathbf{h} | \mathbf{x}) \cdot \mathcal{I}_{bd}(\mathbf{h} | \mathbf{x}) + \mathcal{I}_{ad}(\mathbf{h} | \mathbf{x}) \cdot \mathcal{I}_{bc}(\mathbf{h} | \mathbf{x})$ follows from the variational definition Eq. (13). For instance, for the minimum eigenvalue,

$$\begin{aligned}&\inf_{\mathbf{u}: \|\mathbf{u}\|_2=1} \mathbf{u}^a \mathbf{u}^b \mathbf{u}^c \mathbf{u}^d (\mathcal{I}_{ac}(\mathbf{h} | \mathbf{x}) \cdot \mathcal{I}_{bd}(\mathbf{h} | \mathbf{x}) + \mathcal{I}_{ad}(\mathbf{h} | \mathbf{x}) \cdot \mathcal{I}_{bc}(\mathbf{h} | \mathbf{x})) \\ &= 2 \cdot \inf_{\mathbf{u}: \|\mathbf{u}\|_2=1} \|\mathbf{u}\|_2^2 \\ &= 2.\end{aligned}$$

The maximum eigenvalue is proven identically. \square

Q Proof of Theorem 5.2

We first prove the following corollary which connects the maximum eigenvalues of $\mathcal{K}(\mathbf{t} | \mathbf{x})$ to the maximum eigenvalues of $\mathcal{I}(\mathbf{h} | \mathbf{x})$.

Corollary Q.1. *Suppose that the exponential family in Eq. (1) is specified by a categorical distribution. Then,*

$$\tilde{\lambda}_{\max}(\mathcal{K}(\mathbf{t} | \mathbf{x})) \leq 2 \cdot \lambda_{\max}(\mathcal{I}(\mathbf{h} | \mathbf{x})). \quad (36)$$

Proof. As we are consider a categorical distribution we have that

$$\mathbf{v}_i = \begin{cases} 1 - \sigma_i(\mathbf{h}) & \text{if } y = i \\ 0 - \sigma_i(\mathbf{h}) & \text{if } y \neq i \end{cases}.$$

Thus we have that $|\mathbf{v}_i| \leq 1$. Furthermore, note that the maximum ℓ_2 -norm that we can have is $\|\mathbf{v}\|_2 \leq \sqrt{2}$. Note that this is tight when the positive and negative mass are placed only two distinct coordinates, *i.e.*, $(-1, 1, \dots)$.

Thus using Proposition 4.3, the result follows. \square

Now by using Corollaries 4.2 and Q.1, the remainder of the proof, all we require is the bounding of $\lambda_{\max}(\mathcal{I}(\mathbf{h} | \mathbf{x}))$.

Proof. The first term in the maximum eigenvalue follows from,

$$\begin{aligned}\lambda_{\max}(\mathcal{I}(\mathbf{h} | \mathbf{x})) &= \lambda_{\max}(\text{diag}(\sigma(\mathbf{x})) - \sigma(\mathbf{x})\sigma(\mathbf{x})^\top) \\ &\leq \lambda_{\max}(\text{diag}(\sigma(\mathbf{x}))) - \lambda_{\min}(\sigma(\mathbf{x})\sigma(\mathbf{x})^\top) \\ &= \max_k \sigma_k(\mathbf{x}).\end{aligned}$$

The second term in the maximum follows from the trace of $\mathcal{I}(\mathbf{h} | \mathbf{x})$ being the sum of total eigenvalues. \square

R Proof of Lemma 6.1

Proof. The proof follows from the standard definition of covariance. Denoting $\hat{\boldsymbol{\eta}}(\mathbf{x}) := \mathbb{E}_{q(\mathbf{y}|\mathbf{x})}[\mathbf{t}(\mathbf{y})]$, we have:

$$\text{Cov}^q(\mathbf{t}|\mathbf{x}) = \mathbb{E}_{q(\mathbf{y}|\mathbf{x})}[\mathbf{t}(\mathbf{y})\mathbf{t}^\top(\mathbf{y})] - \hat{\boldsymbol{\eta}}(\mathbf{x})\hat{\boldsymbol{\eta}}^\top(\mathbf{x}).$$

Also expanding $\mathbf{I}(\mathbf{h}|\mathbf{x})$:

$$\begin{aligned} \mathbf{I}(\mathbf{h}|\mathbf{x}) &= \mathbb{E}_{q(\mathbf{y}|\mathbf{x})}[(\mathbf{t}(\mathbf{y}) - \boldsymbol{\eta}(\mathbf{x}))(\mathbf{t}(\mathbf{y}) - \boldsymbol{\eta}(\mathbf{x}))^\top] \\ &= \mathbb{E}_{q(\mathbf{y}|\mathbf{x})}[\mathbf{t}(\mathbf{y})\mathbf{t}^\top(\mathbf{y})] - \boldsymbol{\eta}(\mathbf{x})\hat{\boldsymbol{\eta}}^\top(\mathbf{x}) - \hat{\boldsymbol{\eta}}^\top(\mathbf{x})\boldsymbol{\eta}^\top(\mathbf{x}) + \boldsymbol{\eta}(\mathbf{x})\boldsymbol{\eta}^\top(\mathbf{x}). \end{aligned}$$

Thus we have

$$\begin{aligned} \text{Cov}^q(\mathbf{t}|\mathbf{x}) &= \mathbf{I}(\mathbf{h}|\mathbf{x}) + \boldsymbol{\eta}(\mathbf{x})\hat{\boldsymbol{\eta}}^\top(\mathbf{x}) + \hat{\boldsymbol{\eta}}^\top(\mathbf{x})\boldsymbol{\eta}^\top(\mathbf{x}) - \boldsymbol{\eta}(\mathbf{x})\boldsymbol{\eta}^\top(\mathbf{x}) - \hat{\boldsymbol{\eta}}(\mathbf{x})\hat{\boldsymbol{\eta}}^\top(\mathbf{x}) \\ &= \mathbf{I}(\mathbf{h}|\mathbf{x}) - (\boldsymbol{\eta}(\mathbf{x}) - \hat{\boldsymbol{\eta}}(\mathbf{x}))(\boldsymbol{\eta}(\mathbf{x}) - \hat{\boldsymbol{\eta}}(\mathbf{x}))^\top. \end{aligned}$$

As required. \square

S Proof of Corollary F.1

Proof. We calculate the variance:

$$V(\theta_i) = \frac{1}{N} \left(\mathbb{E}_{q(\mathbf{y}|\mathbf{x})} \left[\left(\frac{\partial \log p(\mathbf{y}|\mathbf{x})}{\partial \theta_i} \right)^2 \right] - \mathbb{E}_{q(\mathbf{x},\mathbf{y})} \left[\frac{\partial \log q(\mathbf{y}|\mathbf{x})}{\partial \theta_i} \right]^2 \right).$$

Each of the terms can be calculated: Let $\boldsymbol{\delta}_a(\mathbf{x}, \mathbf{y}) := (\mathbf{t}(\mathbf{y}) - \boldsymbol{\eta}(\mathbf{x}))$.

$$\begin{aligned} &\mathbb{E}_{p(\mathbf{x},\mathbf{y})} \left[\left(\frac{\partial \log p(\mathbf{y}|\mathbf{x})}{\partial \theta_i} \right)^2 \right] \\ &= \mathbb{E}_{q(\mathbf{y}|\mathbf{x})} \left[\frac{\partial \mathbf{h}^a(\mathbf{x})}{\partial \theta_i} \frac{\partial \mathbf{h}^b(\mathbf{x})}{\partial \theta_i} \frac{\partial \mathbf{h}^c(\mathbf{x})}{\partial \theta_i} \frac{\partial \mathbf{h}^d(\mathbf{x})}{\partial \theta_i} \boldsymbol{\delta}_a(\mathbf{x}, \mathbf{y}) \boldsymbol{\delta}_b(\mathbf{x}, \mathbf{y}) \boldsymbol{\delta}_c(\mathbf{x}, \mathbf{y}) \boldsymbol{\delta}_d(\mathbf{x}, \mathbf{y}) \right] \\ &= \frac{\partial \mathbf{h}^a(\mathbf{x})}{\partial \theta_i} \frac{\partial \mathbf{h}^b(\mathbf{x})}{\partial \theta_i} \frac{\partial \mathbf{h}^c(\mathbf{x})}{\partial \theta_i} \frac{\partial \mathbf{h}^d(\mathbf{x})}{\partial \theta_i} \mathbb{E}_{q(\mathbf{y}|\mathbf{x})} [\boldsymbol{\delta}_a(\mathbf{x}, \mathbf{y}) \boldsymbol{\delta}_b(\mathbf{x}, \mathbf{y}) \boldsymbol{\delta}_c(\mathbf{x}, \mathbf{y}) \boldsymbol{\delta}_d(\mathbf{x}, \mathbf{y})] \\ &= \frac{\partial \mathbf{h}^a(\mathbf{x})}{\partial \theta_i} \frac{\partial \mathbf{h}^b(\mathbf{x})}{\partial \theta_i} \frac{\partial \mathbf{h}^c(\mathbf{x})}{\partial \theta_i} \frac{\partial \mathbf{h}^d(\mathbf{x})}{\partial \theta_i} \mathbf{K}_{abcd}(\mathbf{t}|\mathbf{x}). \end{aligned}$$

And:

$$\begin{aligned} &\mathbb{E}_{p(\mathbf{y}|\mathbf{x})} \left[\frac{\partial \log p(\mathbf{y}|\mathbf{x})}{\partial \theta_i} \right]^2 \\ &= \mathbb{E}_{p(\mathbf{y}|\mathbf{x})} \left[\frac{\partial \mathbf{h}^a(\mathbf{x})}{\partial \theta_i} \frac{\partial \mathbf{h}^b(\mathbf{x})}{\partial \theta_i} \boldsymbol{\delta}_a(\mathbf{x}, \mathbf{y}) \boldsymbol{\delta}_b(\mathbf{x}, \mathbf{y}) \right]^2 \\ &= \left[\frac{\partial \mathbf{h}^a(\mathbf{x})}{\partial \theta_i} \frac{\partial \mathbf{h}^b(\mathbf{x})}{\partial \theta_i} \mathbb{E}_{p(\mathbf{y}|\mathbf{x})} [\boldsymbol{\delta}_a(\mathbf{x}, \mathbf{y}) \boldsymbol{\delta}_b(\mathbf{x}, \mathbf{y})] \right]^2 \\ &= \left[\frac{\partial \mathbf{h}^a(\mathbf{x})}{\partial \theta_i} \frac{\partial \mathbf{h}^b(\mathbf{x})}{\partial \theta_i} \mathbf{I}_{ab}(\mathbf{h}|\mathbf{x}) \right]^2. \end{aligned}$$

Together with Lemma 6.1 proves the theorem. □

T Proof of Corollary E.2

Proof. The proof follows identically to that of Theorem 4.7 with densities changed. □

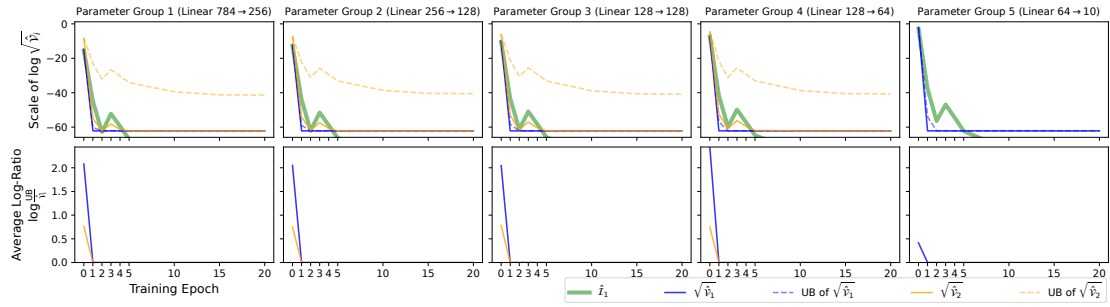


Figure V: The Fisher information, its variances and bounds of the variances w.r.t. a 5-layer MLP with log-sigmoid activation.

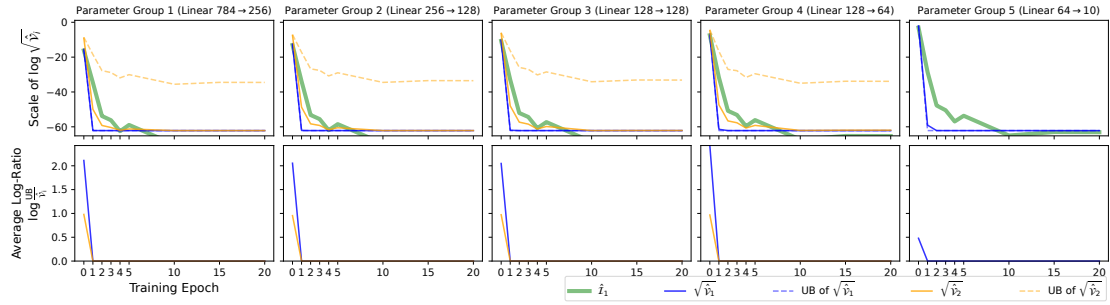


Figure VI: The Fisher information, its variances and bounds of the variances w.r.t. a 5-layer MLP with log-sigmoid activation.

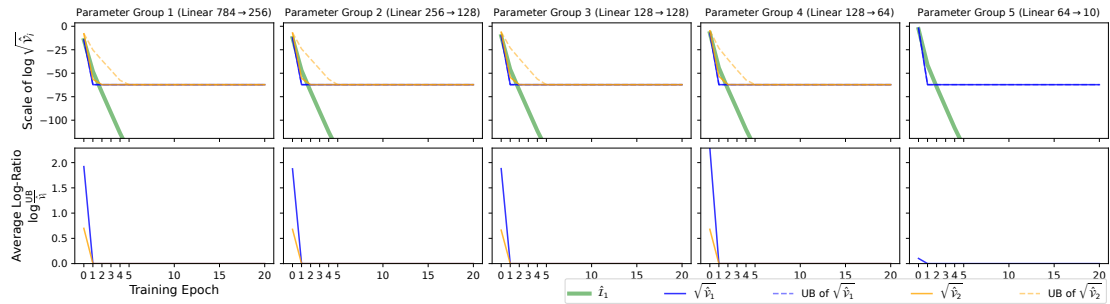


Figure VII: The Fisher information, its variances and bounds of the variances w.r.t. a 5-layer MLP with log-sigmoid activation.

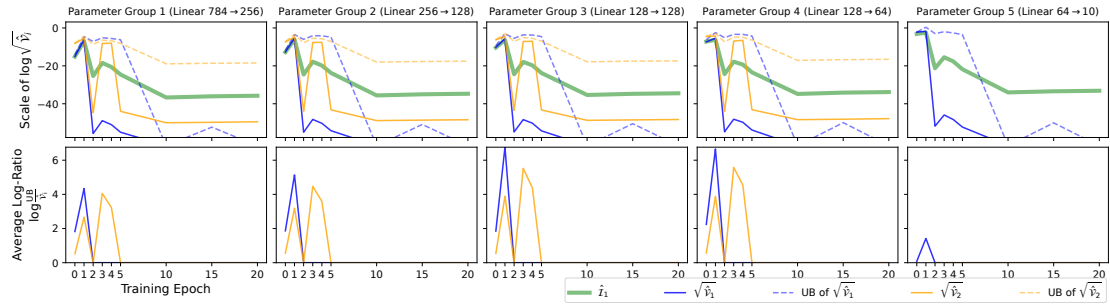


Figure VIII: The Fisher information, its variances and bounds of the variances w.r.t. a 5-layer MLP with log-sigmoid activation.

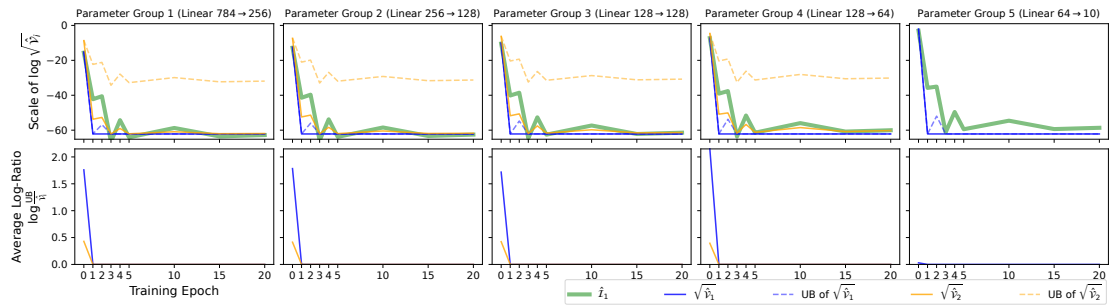


Figure IX: The Fisher information, its variances and bounds of the variances w.r.t. a 5-layer MLP with log-sigmoid activation.